Materials Today Bio 19 (2023) 100559

Contents lists available at ScienceDirect

Materials Today Bio

journal homepage: www.journals.elsevier.com/materials-today-bio

Emerging nanosonosensitizers augment sonodynamic-mediated antimicrobial therapies

Qinglin Xu [a,1], Weijun Xiu [b,1], Qiang Li [a], Yu Zhang [a], Xiaoye Li [a], Meng Ding [a], Dongliang Yang [c,***], Yongbin Mou [a,**], Heng Dong [a,*]

[a] Nanjing Stomatological Hospital, Medical School of Nanjing University, 30 Zhongyang Road, Nanjing, 210008 Jiangsu, PR China
[b] State Key Laboratory for Organic Electronics and Information Displays, Jiangsu Key Laboratory for Biosensors, Institute of Advanced Materials (IAM), Nanjing University of Posts and Telecommunications, Nanjing, Jiangsu 210023, PR China
[c] Key Laboratory of Flexible Electronics (KLOFE) and Institute of Advanced Materials (IAM), School of Physical and Mathematical Sciences, Nanjing Tech University (NanjingTech), Nanjing 211816, China

ARTICLE INFO

Keywords:
Sonodynamic therapy
Antibacterial agents
Nanomaterials
Bacterial infections
Sonosensitizers

ABSTRACT

With the widespread prevalence of drug-resistant pathogens, traditional antibiotics have limited effectiveness and do not yield the desired outcomes. Recently, alternative antibacterial therapies based on ultrasound (US) have been explored to overcome the crisis of bacterial pathogens. Antimicrobial sonodynamic therapy (aSDT) offers an excellent solution that relies on US irradiation to produce reactive oxygen species (ROS) and achieve antibiotic-free mediated antimicrobial effects. In addition, aSDT possesses the advantage of superior tissue penetrability of US compared to light irradiation, demonstrating great feasibility in treating deep infections. Although existing conventional sonosensitizers can produce ROS for antimicrobial activity, some limitations, such as low penetration rate, nonspecific distribution and poor ROS production under hypoxic conditions, result in suboptimal sterilization in aSDT. Recently, emerging nanosonosensitizers have enormous advantages as high-performance agents in aSDT, which overcome the deficiencies of conventional sonosensitizers as described above. Thus, nanosonosensitizer-mediated aSDT has a bright future for the management of bacterial infections. This review classifies the current available nanosonosensitizers and provides an overview of the mechanisms, biomedical applications, recent advances and perspectives of aSDT.

1. Introduction

Due to the rapid spread of drug-resistant bacteria, the efficiencies of traditional antibiotic antimicrobial treatments are limited [1]. Bacteria usually exist in the form of biofilms. Bacteria can adhere to inert or biological surfaces and enclose themselves in extracellular polymeric substances (EPS), including proteins, exopolysaccharides, and extracellular DNA (eDNA) [2]. EPS provide a physical barrier to inhibit the penetration of antibiotics and extremely limit the effects of antibiotics. In addition, the increased prevalence of multidrug-resistant bacterial strains means fewer antibiotics are available to treat bacterial infections [3]. The mechanisms of resistance to antibiotics in multi-resistant bacteria include intrinsic resistance and acquired or developed antibiotic resistance by the bacteria [4]. Although pharmacological modifications or structural optimizations of antibiotics exhibit improved antimicrobial efficacy against bacterial infections, widespread adoption of these new antibiotics into clinical practice seems unlikely in the short term due to expensive and lengthy discovery, development and clinical trial timelines. Therefore, it is urgent to develop non-antibiotic approaches to treat antibiotic-resistant bacterial infections.

Photodynamic therapy (PDT) has long been used in the clinical antimicrobial field [5–11]. It has been confirmed that the illumination of photosensitizers can lead to the inactivation of pathogens through the production of highly reactive oxygen species (ROS) for oxidative damage to lipids, proteins, and genetic materials [12–14]. Typically, the long wavelengths of red light in the visible spectrum have a tissue penetration

* Corresponding author.
** Corresponding author.
*** Corresponding author.
E-mail addresses: yangdl1023@njtech.edu.cn (D. Yang), yongbinmou@nju.edu.cn (Y. Mou), dongheng90@smail.nju.edu.cn (H. Dong).
[1] Qinglin Xu and Weijun Xiu contributed equally to this work.

https://doi.org/10.1016/j.mtbio.2023.100559
Received 10 November 2022; Received in revised form 7 January 2023; Accepted 19 January 2023
Available online 21 January 2023

depth of only a few millimeters, and the longer wavelengths of NIR light minimize tissue scattering and can only penetrate to a depth of approximately 1 cm; thus, PDT is not sufficient for the treatment of deep tissue infections [15]. Recently, developing two-photon (TP) and NIR light response photosensitizers can improve the effects of PDT; however, the weak permeability to the deep site of infection has not been addressed because TP excitation requires almost simultaneous absorption of two coherent near-infrared photons, which depend on expensive pulsed lasers [16–18]. Ultrasound (US) is a mechanical wave with periodic vibration of particles in a continuous elastic medium with a frequency equal to or greater than 20 kHz [19]. It was found that the acoustic field cannot be coupled directly to the energy levels of the molecules. Therefore, US irradiation is considered to be a safe treatment method that has excellent tissue penetration without significant energy attenuation [20]. Sonodynamic therapy (SDT) refers to sonochemical or sonophotochemical events in the acoustic field that result in cytotoxicity dependent on the sensitizer [21]. US-mediated SDT has already been used as a well-established anti-tumor treatment strategy [22–25], which can promote tumor cell killing by accredited mechanisms, including the generation of ROS and ultrasonic cavitation [26]. Recently, US-mediated SDT has been applied in antimicrobial therapy [27]. In contrast to conventional antibiotic therapy, SDT can generate ROS under US irradiation, which directly results in the death of bacteria without the concern of the emergence of drug resistance. In addition, the main advantage of SDT is that it is more penetrating than PDT, which has a more focused effect on the specific site of infection [28,29]. For example, US can reach deep organs, such as the pancreas and liver. Moreover, SDT in combination with other strategies has been found to have better effects on destroying a wide range of forms of microorganisms, from free bacteria to biofilm [30–33]. Thus, an increasing number of scholars have focused on optimizing antimicrobial sonodynamic therapy (aSDT) [34–36].

Sonosensitizer is an important part of SDT and the ideal sonosensitizer should have a high degree of acoustic sensitivity [37]. When sonosensitizers are exposed to US, they are activated from the ground state to the excited state. The activated sonosensitizers then return to the ground state where they release energy to produce ROS for promoting bacterial damage. However, conventional sonosensitizers, such as small molecules, exhibit problems including poor targeting ability, poor hydrophobicity, low bioavailability, easy production of toxic side effects, rapid excretion and short duration of action. Many traditional sonosensitizers, such as porphyrin-based compounds, curcumin, and rose bengal, are highly hydrophobic, which allows them to be easily eliminated from the blood circulation and results in insufficient accumulation in infected areas. In addition, traditional sonosensitizers have an insufficient utilization efficiency of US energy causing a limited cavitation effect and subsequently failing to sufficiently generate ROS for bacterial inactivation. Moreover, bacterial infection is always accompanied by a hypoxic microenvironment, which further inhibits the antibacterial efficacy of oxygen-dependent aSDT [38]. Currently, the advent and rapid development of nanotechnology have led to a significant change in the biomedical paradigm. Nanomedicine-enabled/augmented nanodynamic therapy is triggered by exogenous or endogenous activators on nanosensitizers and generates active free ROS for nanotherapeutic purposes [39–41]. Nanosonosensitizers refer to small molecule sonosensitizer-loaded nanoparticles or nanomaterials that themselves have acoustic sensitization effects. Nanosonosensitizers can not only be effectively delivered to the site of inflammatory infection [42] but also lower cavitation thresholds and enhanced cavitation effects, thereby improving the efficiency of aSDT [43]. Nanosonosensitizers can also be elaborately engineered for implementing bacteria-targeted sonotheranostics-based bacteria-specific metabolic environment. Some oxygen-generating nanosonosensitizers can relieve the hypoxia barrier of biofilms, which could significantly contribute to promoting the efficiency of aSDT.

This review gives a brief overview of nanosonosensitizers (Fig. 1). In addition, the antimicrobial mechanisms of nanosonosensitizer-mediated

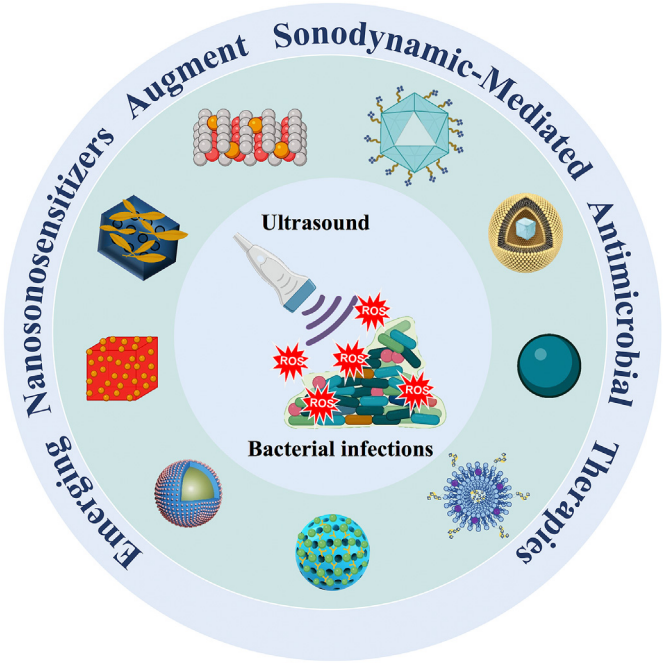

Fig. 1. Nanosonosensitizers in aSDT.

aSDT was discussed. The medical applications of nanosonosensitizers in aSDT/combination therapy for treating different bacterial infectious diseases were summarized. Finally, the current status and future prospects of nanosonosensitizers to meet antibacterial clinical needs are provided.

2. Categories of nanosonosensitizers

Nanosonosensitizers are noted for their high stability, good permeability and biocompatibility. Compared to conventional sonosensitizers, nanosonosensitizers are able to improve hydrophobicity and prolong the circulation time for better accumulation at the site of infection. In addition, nanoscale biomaterials effectively promote the cellular uptake of nanosonosensitizers and allow them to easily penetrate deeper tissues. They can improve the water-solubility and biocompatibility of sonosensitizers without changing their physicochemical properties [44]. In addition, nanosonosensitizers can increase the rate of ultrasonic kinetic deactivation for bacteria [45]. There is a wide range of aSDT-related nanosonosensitizers that can be applied to kill bacteria or destroy biofilms. In terms of form, they can be divided into three categories (Table 1): sonosensitizer nanoparticles (SSNPs), encapsulation of sonosensitizer in nanocarriers (ESSNCs) and conjugation of sonosensitizers with nanocarriers (CSSNCs).

2.1. Sonosensitizer nanoparticles (SSNPs)

SSNPs refer to sonosensitizers that themselves are nanoscale and have the characteristics of not only nanomaterials but also sonosensitizers. The most common nanosonosensitizers are metallic oxide nanoparticles. For example, zinc oxide nanoparticles (ZnO NPs) and titanium dioxide nanoparticles (TiO_2 NPs) are effective as nanosonosensitizers for synergistic bactericidal effects on *Streptococcus mutans* biofilms under US irradiation [46]. In addition, metal peroxide nanoparticles possess intrinsic physicochemical characteristics and unique biological functions, which satisfy the requirements of aSDT. Silver peroxide nanoparticles (Ag_2O_2 NPs) can be considered both oxidizing and reducing agents and have enhanced antibacterial and antibiofilm capabilities *via* ROS production and cavitation microbubbles [50]. The aSDT entirely depends on ROS generation. SSNPs can be activated by US, and its

Table 1
Representative nanosonosensitizers in aSDT.

Nanosonosensitizers	Parameters of Ultrasound	Dose	Microorganism	Anti-bacterial effects of aSDT	Ref.
SSNPs					
ZnO NPs, TiO_2 NPs, and ZnO/TiO_2 NPs	0.75 W/cm^2, 1 MHz, 1 min	Sub-significant reduction dose: 3.1 μg/mL, 25 μg/mL, and 1.5 μg/mL, respectively	*S. mutans*, *S. mutans* biofilm	5.8 Log_{10} CFU/mL (99.999984% reduction), 6.3 Log_{10} CFU/mL (99.999994% reduction), and 7.9 Log_{10} CFU/mL (99.999996% reduction), respectively	[46]
RBC-Au@Cu_2O hybrid nanocubes	1.5 W/cm^2, 1 MHz, 50% cycle, 15 min	0.25 mg/mL	*S. aureus* planktonic	99.67% reduction	[47]
DSiNPS	1 MHz, 1 W/cm^2, 10 min	1 mg/mL	*E. coil* planktonic	Drop in the viability up to 72%	[48]
Ti–S–$TiO_{2\text{-}X}$*	1 MHz, 1.5 W/cm^2, 50% cycle, 15 min	NA; implant coatings	*S. aureus* planktonic	Antibacterial efficiency of Ti–S–$TiO_{2\text{-}X}$ + US, and Ti–S–$TiO_{2\text{-}X}$ + Light + US were calculated to be 71.517%, and 99.995%, respectively.	[49]
Ag_2O_2 NPs*	1 W/cm^2, 1 MHz, 10 min	100 μg/mL	MRSA, *S. aureus*, *E. coli*, *P. aeruginosa* planktonic	The killing rate >99.99% under US, and killing rate >99.9999% under US + NIR	[50]
ESSNCs					
N-EMO	1 MHz, 2 W/cm^2, 5 min	0.03×10^{-4} g/L~20 $\times 10^{-4}$ g/L	Biofilms (*S. aureus*, *P. aeruginosa*, *A. baumannii*)	Inhibiting the biofilm growth of multi-species test bacteria by 5.725 ± 0.12 (99.9993%).	[51]
MLP18	1 MHz, 0.97 W/cm^2, 5 min	20 μM purpurin 18	*E. coli*/MRSA planktonic	Obvious growth inhibition upon US activation	[52]
AVNs–TPPS	1 MHz, 0.97 W/cm^2, 50% cycle, 8 min	200 μg/mL	MRSA	Complete eradication of MRSA infection	[53]
AmB-NPs	42 kHz, 0.3 W/cm^2, 15 min	12.5 μg/mL	*C. albicans*	The sterilization rate was 99.65%	[54]
Cur-NisNp*	1 MHz, 45.2 mW/cm^2, 1 min	15.6 μg/mL	*A. baumannii* biofilm	Significantly reducing the *A. baumannii* biofilm under US + LED	[55]
CNPS-ICG*	1 MHz, 1.56 W/cm^2, 1 min	1000 μg/mL	Biofilms (*P. gingivalis*, *Prevotella intermedia*)	Removed periopathogens biofilm on the surface of titanium dental implant under diode laser irradiation + US	[56]
CSSNCs					
HFH@ZIF-8	0.5 MHz, 1.2 W/cm^2, 50% cycle, 10 min	100 μg/mL *in vitro*; 5 mg/kg *in vivo*	MRSA	Significant inhibition of the vitality of MRSA	[57]
RBC-HNTM-Pt@Au	1 MHz, 1.5 W/cm^2, 50% cycle, 15 min	400 μg/mL *in vitro*; 1 mg/mL *in vivo*	MRSA	Antibacterial effect was 99.93%	[58]
Pd@Pt-T790	1 MHz, 0.97 W/cm^2, 50% cycle, 8 min	50 ppm	MRSA	Nearly 100% of bacteria were killed	[59]
M@P–Fe	1 MHz, 0.5 W cm/^{2}, 3 min	100 μg/mL	*E. faecalis*	The biofilm eradication in root canal	[60]
IR780@PLGA	1 MHz, 2 W/cm^2, 50% cycle, 30 s on and 30 s off for four on/off cycles	10.0 mg/mL, each 100 μL	MRSA planktonic and biofilm	Bacteria were almost completely obliterated and biofilm was eliminated and broken into pieces	[61]
NM@Cur	1 MHz, 1.56 W/cm^2, 1 min	50 mM	*S. mutans*	Decreased the cell viability to 99.9%	[62]
PPPCs	1 MHz, 1.5 W/cm^2, 9 min	$C_{MnTCPP} = 3 \times 0.04$ mM	MRSA	Achieved the precise and effective treatment for deep infections	[63]
Fe@UCNP-HMME*	2 W/cm^2, 10 min	125 μg/mL	*E. coli*/MRSA	Achieved 0% of relative viability	[64]

Abbreviation: *means photo/sonodynamic synergetic nanoagents; SSNPs, sonosensitizer nanoparticles; ESSNCs, encapsulation of sonosensitizers in nanocarriers; CSSNCs, conjugation of sonosensitizers with nanocarriers; ZnO NPs, zinc oxide nanoparticles; TiO_2 NPs, titanium dioxide nanoparticles; RBC-Au@Cu_2O, red blood cell membrane coating aurum-cupric oxide; DSiNPS, polysaccharide (dextran)-coated silica nanoparticles; Ti–S–TiO_2-X, titanium-sulfur-doping; Ag_2O_2 NPS, silver peroxide nanoparticles; N-EMO, nano-emodin; MLP18, maltohexaose-modified cholesterol-phospholipid-purpurin 18; Cur-NisNP, Curcumin-Nisin-based poly (L-lactic acid) nanoparticle; CNPS-ICG, chitosan nanoparticles-indocyanine green; HFH@ZIF-8, hematoporphyrin monomethyl ether-zeolitic imidazolate framework-8; RBC-HNTM-Pt@Au, red cell membrane-zirconium based porphyrin metal−organic framework-platinum-aurum; Pd@Pt-T790, palladium-platinum-*meso*-tetra(4-carboxyphenyl) porphine; M@P–Fe, mesoporous silica nanoparticles-protoporphyrin IX-iron ions; IR780@PLGA, IR780 iodide-lactic-co-glycolic acid; NM@Cur, nanomicelle curcumin; PPPC, polymer-peptide-porphyrin conjugate; UCNPS, yolk-structured multifunctional upconversion nanoparticles; Fe@UCNP-HMME, ferrum-upconversion nanoparticles-hematoporphyrin monomethyl ether.

mechanism relies on the jump of exciting electrons from their valence band (VB) to the conduction band (CB). However, rapid recombination of electrons and holes impedes the generation of ROS. Zhu et al. designed red blood cell (RBC) membranes coated with Au@Cu_2O hybrid nanocubes [47]. They synthesized Au as the metal catalyst and Cu_2O as its semiconductor counterpart and found a Schottky contact at the post-synthesis interface, which can be demonstrated by the peak shift shown by the X-ray photoelectron spectroscopy (XPS) results. Under US stimulation, electrons of Cu_2O are excited from their VB to the CB, the edge of which is above the Fermi level of Au. In addition, the Schottky barrier prevents the return of electrons and promotes electron-hole separation. The above process facilitates the reaction of H_2O and O_2 to produce ROS, which results in 99.67% of *S. aureus* being killed by US irradiation for 15 min. These results showed the excellent antibacterial effects of SSNPs under US irradiation.

2.2. Encapsulation of sonosensitizer in nanocarriers (ESSNCs)

Most conventional sonosensitizers are themselves small molecule compounds, which limits their ability to penetrate deep infection tissues. Therefore, researchers have attempted to encapsulate small molecule sonosensitizers in nanoparticles to facilitate *in vivo* delivery. The sonosensitizers can be physically loaded in the nanoparticle substrate, which can increase the hydrophilicity of sonosensitizers and promote the rapid infiltration of ESSNCs into deeply infected tissues. Numerous ESSNCs possess outstanding properties, including powerful entrapment efficiency, high biocompatibility, and stability in diverse physiological conditions. Most encapsulation methods are based on the precipitation process of sonosensitizers. Sedimentation efficiency can be optimized by adding a nonsolvent or changing the physicochemical parameters, such as the pH, salinity or temperature [65]. The encapsulation process mostly

relies on non-covalent bonding between sonosensitizers and nanocarriers. For example, Pourhajibagher et al. prepared self-assembled nano-emodin (N-EMO), which was formed by a host-guest interaction between the Gel-CD copolymer and EMO [51]. The aSDT using N-EMO might decrease biofilm formation of multi-species bacterial biofilms in burn wound infections. Yang et al. prepared amphotericin B-loaded nanoparticles (AmB-NPs) by a poly (lactic-*co*-glycolic acid) PLGA double emulsion method [54]. Notably, some ESSNCs can modify erythrocyte membranes through non-covalent bonding (*i.e.,* electrostatic adsorption) to improve their biocompatibility [47,58]. Moreover, parts of sonosensitizers act not only as US-responsive bactericidal agents but also as optical imaging agents for aSDT-based visualization. Purpurin 18 (P18), a porphyrin structural molecule, is a sonosensitizer with unique luminescent properties that can potently overcome tissue absorption and scattering. However, some fundamental limitations of P18, including high hydrophobicity, ease of auto quenching, and poor bacterial specificity, need to be resolved. Xu and coworkers encapsulated P18 into nanoliposomes (MLP18) as ESSNCs, which efficiently released and internalized P18 into bacteria and allowed *in situ* visualization of the infection area [52]. Inspired by advances in encapsulation technology, enhancing aSDT by nanoengineering ESSNCs may be a potential solution.

2.3. Conjugation of sonosensitizers with nanocarriers (CSSNCs)

Conjugation of sonosensitizers with nanoparticles is another way to promote SDT efficiency. Sonosensitizer-conjugated nanoparticles are constructed by a covalent combination of the two components. There are usually two construction methods: one is that sonosensitizers are chemically bound to the surface of nanoparticles, and the other is that sonosensitizers chemically attach to the polymer backbone and the complex subsequently self-assembles into nanoparticles [57,59,63]. CSSNCs provide an emerging and reliable idea for the development of novel agents to promote the effects of aSDT. Here are some examples of composites connected by covalent bonds. Wang et al. designed novel TiO_2-based CSSNCs (named DFT), which were synthesized by TiO_2 nanocarriers conjugated with a porphyrin sensitizer-DVDMS [66]. DFT achieved an eradication efficiency of 92.4% for *S. aureus* under US irradiation. Geng et al. loaded the sonosensitizer hematoporphyrin monomethyl ether (HMME) into the porous material zeolitic imidazolate framework-8 (ZIF-8) to form H@ZIF-8 nanoparticles by linking metal ions with organically bound ligands, and then the HFH@ZIF-8 nanoplatform was constructed by modifying H@ZIF-8 nanoparticles with F127 and hemoglobin through electrostatic incorporation [57]. HFH@ZIF-8 exhibited enhanced water-solubility, good biocompatibility, and improved disease-targeting capability for delivering and releasing sonosensitizers. More interestingly, the presence of hemoglobin in HFH@ZIF-8 can offer sufficient oxygen consumption by SDT and relieve hypoxia inhibition of deep infection. It follows that in the process of constructing CSSNCs, different chemical bonds can be used to provide suitable connections for achieving the coordinated action of the constituent elements of the sonosensitizer platform.

Research studies on novel nanosonosensitizers provide a way to improve the therapeutic effectiveness of aSDT. SSNPs exploit their inherent advantage of making the nanoparticles an active participant in sonosensitizer delivery rather than a passive carrier. For ESSNCs, the encapsulation protects the sonosensitizer located inside from the harmful external environment, and the stability of the nanoparticles can be easily tailored to further protect the sonosensitizer from degradation. Compared with encapsulation, the main advantages of CSSNCs are sustained drug release, higher drug loading, and better stability without undesirable leakage. Researchers can design suitable agents according to their requirements based on the advantages of different categories of sonosensitizers.

3. Potential antimicrobial mechanisms during US stimulation

The bacterial cell envelope has three important signal sequence targets, including cell membrane phospholipids, proteins, and nucleic acids [67]. By disrupting these targets, US stimulation can induce morphological and functional changes in microbial cells [68]. Morphological damage mainly consists of changes in the structure of the mesosome. Direct damage to the cell wall and intracellular membrane of bacteria disrupts the integrity of the cell membrane, leading to leakage of cytoplasmic contents and consequent inactivation of the cell membrane transport system [69]. Alterations in function are usually caused by disturbances in membrane potential, loss of protein and enzyme activity, and inhibition of metabolic processes (*e.g.*, DNA replication, glucose transport) [70,71]. Gram-positive and gram-negative bacteria differ in their reactivity to aSDT. Gram-positive bacteria are more sensitive to aSDT because the thick but porous peptidoglycan layer facilitates the entry of nanosonosensitizers [72,73]. In contrast, gram-negative bacteria have a strong barrier due to their complex cell wall structure, and therefore, sonosensitizers can only bind to the cell wall [45]. Nonetheless, the possibility of enhancing the antimicrobial effect with cationic sonosensitizers has been suggested based on the fact that negatively charged phosphate groups on the outer membrane of gram-negative bacteria facilitate the binding of cationic sensitizers [73–75]. This finding prompts us to consider not only the target points for killing bacteria when performing antibacterial tests, but also to design the appropriate nanosonosensitizer according to the bacterial structure. In addition, biofilms are the main form in which bacteria exist and function, which results in high drug tolerance for bacteria within biofilms [76–78]. Biofilms are aggregated bacterial populations that are usually encapsulated with EPS. The self-secreted EPS around biofilms provides a physical barrier for bacteria to restrict sonosensitizer penetration and the effects of aSDT. Thus, highly desired nanosonosensitizers are available clinically to control and treat biofilms.

Currently, the widely accepted antibacterial mechanism of aSDT is the generation of ROS [20]. In addition, the physical damage caused to bacteria by the energy generated by US irradiation also assists the antimicrobial efficiency of aSDT, to some extent [79]. In this section, we will discuss these potential antimicrobial mechanisms during US stimulation, including the generation of ROS in nanosonosensitizer-mediated aSDT and the auxiliary antimicrobial mechanisms during US irradiation.

3.1. Generation of ROS by nanosonosensitizers in aSDT

Numerous experiments have demonstrated that US can stimulate the production of ROS by sonosensitizers [20,80–82]. When certain forms of sonosensitizers or endogenous molecules are exposed to US, compounds are activated from their ground state to the excited state. The activated compounds then return to the ground state, and the energy they release can generate ROS, which directly mediate bacterial damage (Fig. 2A). When sufficient ROS are generated, the bacteria will activate a series of events that ultimately lead to apoptosis [21,62,83]. The generation of ROS is considered an effective way for nanosonosensitizers to mediate the bactericidal effect. In addition, there are two hypotheses for the mechanism of ROS production during acoustic stimulation of nanosonosensitizers: the sonoluminescence hypothesis and the pyrolysis hypothesis. Some scholars have demonstrated that ultrasonically irradiated liquids produce light, which is the basis of the sonoluminescence hypothesis [84–86]. The bubbles generated within the liquid will appear as light during the burst collapse and subsequently stimulate the nanosonosensitizers to produce ROS. The exact mechanism of the process has not been elucidated, but it is widely accepted that it may be related to blackbody radiation, bremsstrahlung, or recombination radiation [86]. The pyrolysis hypothesis is another mechanism by which sonosensitizers

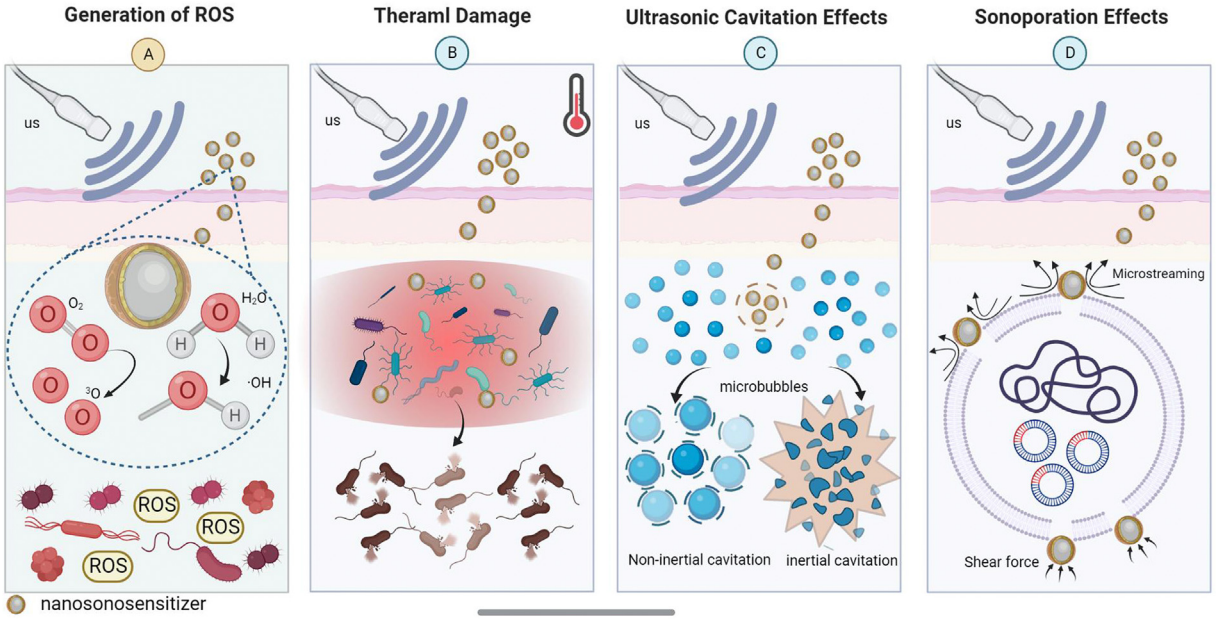

Fig. 2. Potential antimicrobial mechanisms during US stimulation. (A) Generation of ROS. ROS generated in response to US can be directly involved in mediating cytotoxicity. ROS have a large diffusion radius and can cross the mitochondrial membrane, participating in electron transfer and oxidation, thus affecting the mitochondrial respiratory chain of bacteria. (B) Thermal damage. US irradiation of nanosonosensitizers increases the temperature, and the bacteria are killed directly when the temperature rises under US irradiation. (C) Ultrasonic cavitation effects. A rapid increase in mechanical pressure caused by the acoustic energy of nanosonosensitizers under US irradiation, results in the creation of microbubbles in the tissue fluid, disrupting the cytoskeleton, cell membranes and the activity of biological enzymes. (D) Sonoporation effects. Under the induction of US, temporary pores are created in the cell membrane of bacteria, thus facilitating the penetration of more nanosonosensitizers into the cells.

produce ROS when induced by US. When US hits the liquid, bubbles appear, which gradually become larger and eventually explode. The process generates a temporary heat, raising the surrounding temperature and prompting the pyrolyzed nanosonosensitizers to react with oxygen and generate ROS [87,88].

3.2. Auxiliary antimicrobial mechanisms during US irradiation

3.2.1. Thermal damage

Several strategies have been reported to suppress bacterial infections *via* thermal damage, such as photothermal therapy (PTT) and magnetothermal therapy [89,90]. Similarly, US can convert mechanical vibration energy into thermal energy for antimicrobial effects (Fig. 2B) [91]. However, the excess heat generated in the infected tissues tends to damage host tissues and prolong the healing time. In addition, the absorption, attenuation and scattering of sound waves along the acoustic channel can lead to insufficient energy deposition, while the problems of diffusion and loss of thermal energy can make the conversion of mechanical energy to thermal energy inefficient [92]. Thus, thermal damage is not yet the main antibacterial mechanism of aSDT.

3.2.2. Ultrasonic cavitation effects

The ultrasonic cavitation effect is the rapid increase in mechanical pressure caused by the acoustic energy from US, resulting in the creation of microbubbles in the tissue fluid [93]. This process involves growth, nucleation and oscillation of gaseous cavities [94]. Cavitation can be divided into two modes (Fig. 2C): inertial cavitation and noninertial cavitation (stable cavitation) [95]. Inertial cavitation refers to the stronger bubble dynamics processes that occur in liquids under high-intensity US. The bubble can contract dramatically until it collapses, absorbing large amounts of acoustic energy. It then releases energy in a very small area, resulting in the formation of a high temperature and pressure environment in this area, along with the formation of strong shock waves, high speed microjets, and free radicals in the liquid [96,97]. Noninertial cavitation occurs in low-temperature liquid media, where the bubbles produced in the process do not collapse as violently as inertial cavitation; it is a slow and gentle process [93,95]. The changes in physicochemical conditions that occur under the influence of the cavitation effect can cause mechanical damage to bacteria and biofilms.

3.2.3. Sonoporation eeffects

Sonoporation relies on US action to create pores in bacteria (Fig. 2D). When exposed to US, the shear stress and microflow generated by acoustic cavitation can increase cell membrane permeability and cause transient pores in the cell membrane of bacteria, resulting in the sonoporation effect [98]. Studies have reported that under US induction, temporary pores are created in the cell membranes of bacteria, thus facilitating the penetration of more nanoscale drugs into the cells [99]. These theories and studies provide a novel idea for us to explore the delivery route of nanosonosensitizers, improve the penetration rate of agents and enhance the antimicrobial effect.

4. The advantages of nanosonosensitizers for promoting aSDT

4.1. High targeting ability of the nanosonosensitizer

The specificity of the sonosensitizer is a critical factor for the bactericidal ability of aSDT *in vivo*. The low specificity of sonosensitizers in the infection area not only limits their therapeutic effectiveness, but also results in complications due to untargeted accumulation in normal tissue [100]. It has been found that bacterial-specific metabolic pathways are often not present in mammalian cells. The ability to precisely distinguish bacterial infections from sterile inflammatory diseases through this pathway certainly provides great help and clues for aSDT-targeted therapy [101]. Therefore, the development of nanosonosensitizers with targeting ability for infected tissues facilitates the enhancement of the antimicrobial effect. Maltodextrin-specific bacteria can be labeled by maltotriose targeting. Through the free-reducing end, the system remains

stable in serum with increased metabolic uptake to enable tracking and amplification of the targeting signal [102]. Inspired by this, Pang et al. developed a bacteria-responsive nanoliposome (MLP18) as a smart sonotheranostic for combating MDR bacterial infections [52]. They encapsulated P18 into the MLP18 nanocomposite, which consisted of maltohexaose-modified cholesterol and DSPG-containing lipid compositions. The prepared MLP18 conjugating a bacteria-targeted ligand of maltohexaose can specifically target the bacteria-infected site of mice. Furthermore, the bacteria-responsive characteristics of MLP18 activated the effective release and internalization of high-concentration sensitizers into the bacterial cells, thereby effectively eliminating MDR bacteria through acoustic kinetics.

In addition, some enzyme-responsive peptides can react with bacteria-secreted gelatinase; therefore, nanosonosensitizers modified with enzyme-responsive peptides can gain bacterial targeting ability. Wang et al. developed a polymer-peptide-porphyrin conjugate (PPPC), which achieves specific enrichment in bacterial infection tissue [63]. PPPC is modified with an enzyme-responsive peptide. When bacteria oversecrete gelatinase, it cuts the enzyme-responsive peptide from PPPC, removing the protective PEG layer and causing the formation of nanoaggregates in the bacterial infection tissue. The results showed that the PPPC group was four times more capable of binding to bacteria than the control group. Accurately distinguishing bacterial infections from other pathological changes is a major challenge that hinders the timely and effective diagnosis of bacterial infections *in vivo*. Further development of bacterial-targeted nanosonosensitizers is a promising way to improve the efficiency of aSDT.

4.2. Overcoming the hypoxic environment of bacteria-infected tissue

Oxygen is essential to the generation of ROS by activated sonosensitizers in aSDT. The hypoxic environment of bacteria-infected tissue restricts the bactericidal efficacy of aSDT to a high degree. In addition, the consumption of oxygen during aSDT may exacerbate the hypoxic state, further contributing to the inefficiency of aSDT [59]. Developments in nanotechnology offer promising ways to solve the dilemma of an oxygen-deficient microenvironment in infected areas. Some common approaches include the development of self-generating oxygen materials and inorganic nanoenzymes (such as catalase and MnO_2). In addition to the hypoxic characteristics of the bacterial infection area, high concentrations of H_2O_2 are often present. These nanoenzymes can promote endogenous H_2O_2 conversion to O_2, which provides sufficient O_2 to facilitate subsequent ROS production in aSDT, and they also alleviate the hypoxic predicament of the infected tissue [70].

In recent years, some novel nanosonosensitizers have been designed to alleviate hypoxia. Hemoglobin has natural biocompatibility, which prolongs the circulation time of nanoparticles in the body and accumulates at the site of infection to take effect. In addition, oxygen-carrying hemoglobin can release oxygen locally, providing sufficient oxygen consumption for the SDT process. Hemoglobin-modified nanosonosensitizer (HFH@ZIF-8) can facilitate the provision of oxygen production *in situ*, which greatly enhances the effects of aSDT by overcoming the barriers of the oxygen-deficient environment [57]. Modification and denaturation of oxygen-producing nanoenzymes is also a hot topic of research. The development of emerging nanosonosensitizers loaded nanoenzymes can achieve disease-site specificity and controlled catalytic activity of nanoenzymes. Sun et al. proposed a switchable nanozyme system (Pd@Pt-T790) for the controlled generation of catalytic oxygen and production of a large amount of ROS during US stimulation, which overcame hypoxia-related barriers and enhanced the efficacy of aSDT [59]. T790 significantly blocked the peroxidase-like activity of Pd@Pt and nanozyme activity was effectively restored under US irradiation (1 MHz, 0.97 W/cm^2, 50% duty cycle, 8 min). Then, restored nanoenzymes catalyzed the breakdown of endogenous H_2O_2 to O_2. These nanosonosensitizers not only precisely regulate the production of O_2 to induce ROS, but also reduce the potential toxicity of the nanoenzyme to normal tissue. Whether applying self-oxygenating materials in hypoxic infected tissue or generating oxygen *in situ* through the reaction of nanoenzymes, both can realize rational O_2 self-replenishment in aSDT.

4.3. Noninvasive monitoring of aSDT

Rapid and accurate diagnosis of bacterial infection is imperative to guide therapeutic regimens and control the spread of this disease. When the drug concentration in the area of the lesion is unknown, it adds to the difficulty of subsequent dosing and is likely to result in overdosing or underdosing. Real-time monitoring of drug concentrations is necessary to maintain an optimal therapeutic window in the infected area of the body. Some nanosonosensitizers can be used as visualization tools by imaging technology. As discussed in the previous section, PPPC can achieve aggregation in infected areas. The combined application of PPPC and magnetic resonance imaging (MRI) allows for factual measurement of sonosensitizer enrichment at the site of infection. Wang and coworkers constructed PPPCs that achieved real-time monitoring at the site of infection by MRI of T1 and T2, which enables precise aSDT [63]. T1 is more favorable for the observation of anatomical structures and T2 is more favorable for the visualization of tissue lesions. The combination of T1 and T2 allows for more effective observation of pathological tissue and precise monitoring of drug concentrations.

In addition, some nanosonosensitizers can realize the diagnosis of bacterial infection by dual-modal imaging. Pd@Pt-T790 can effectively accumulate in the infected site and provide imaging-guided infection monitoring [59]. Comparing *in vivo* PA imaging 6 h after intravenous injection with pre-injection, it was found that the PA signal around the site of infection was nearly two times higher in Pd@pt-treated mice than before the injection. These successful practices for non-invasive monitoring of aSDT show that precise targeting and tracking of bacteria not only enable effective antimicrobial activity, but also guide the dose and frequency of nanosonosensitizer use in clinical practice. Some practices have already experimented with combining targeted antimicrobial therapy and non-invasive monitoring, and in the future, this will be a novel idea to improve the efficiency of aSDT.

5. Applying nanosonosensitizer-mediated aSDT for infectious diseases

5.1. Treatment for skin infections

Infection of burn wounds is often caused by the disruption of skin integrity and the colonization of the damaged wound by microbial flora that are already present in the normal body. Kennedy et al. presented that in burn wounds, gram-positive organisms of the skin parasite colonize the wound, followed by gram-negative organisms and yeasts [103]. Asati et al. found that bacterial biofilms are thought to be responsible for inducing chronic inflammation in these patients, resulting in nonhealing burn wounds [104]. The high rates of biofilm formation and antibiotic resistance found in wounds both make the management of burn wound infections a challenge.

In response to this challenge, Pourhajibagher et al. investigated the antibiofilm efficacy of aSDT using nanoemodin (N-EMO) against multispecies bacterial biofilms containing *S. aureus*, *P. aeruginosa*, and *A. baumannii* [51]. In addition, to assess changes in gene expression in microbial strains, they examined virulence factors associated with biofilm formation. The results showed that the gene expression levels of *lasI*, *agrA* and *abaI* were significantly reduced after US irradiation, and the changes in these parameters were considered to be possibly related to reduced expression levels of transcription factors, genomic stress through microenvironmental modifications, or genomic instability. In conclusion, they confirmed that under US irradiation for 5 min (2 W/cm^2, 1 MHz), N-EMO-mediated aSDT has positive effects on the inhibition of biofilm formation, degradation of formed biofilms and reduction of virulence factors associated with multispecies bacterial biofilms.

In addition, skin abscesses caused by bacterial biofilms can be treated with nanosonosensitizer-mediated aSDT. The matrix encapsulation of EPS in the abscess area creates unique conditions in the biofilm microenvironment, including hypoxia and an acidic pH [105–107]. The treatment of biofilm-associated infections by traditional aSDT is difficult due to the EPS physical barrier inhibiting the penetration of nanosonosensitizers, and the hypoxic microenvironment of biofilms further restricts the sonodynamic efficiency of nanosonosensitizers [108]. Dong et al. constructed a biofilm microenvironment response nanoplatform to degrade the biofilm structure and relieve hypoxia to enhance the biofilm eradication efficiency of aSDT (Fig. 3A–C) [109]. After its delivery into MRSA biofilm-infected sites, MAPC decomposes in the acidic biofilm microenvironment and subsequently releases α-amylase and Ce6 (Fig. 3D). On the one hand, α-amylase can degrade the EPS of MRSA biofilms and further promote Ce6 penetration. On the other hand, MNSs with catalase-like activity can convert overexpressed H_2O_2 into O_2 to relieve the hypoxic biofilm microenvironment, which significantly enhances the sonodynamic efficiency of Ce6. The bacterial inactivation efficiency in MRSA biofilm-infected mice was approximately 5.2 log units (99.9993%) after treatment with MAPC under US stimulation (1 W/cm^2, 1 MHz, 10 min), suggesting the superior biofilm eradication efficiency of combining biofilm structure degradation with improved aSDT brought about hypoxia relief (Fig. 3E).

In the search for sonosensitizers with good biocompatibility and efficient performance, Wu et al. have blazed a new trial by using piezoelectric nanocomposites as novel sensitizers to achieve efficient SDT. Piezoelectric materials have a unique piezoelectric effect, when subjected to external mechanical stress, immediately generates a built-in electric field and surface piezoelectric potential [110]. The piezoelectric potential can be used to catalyse the formation of charge carriers between the metal and the piezoelectric semiconductor, improving the catalytic performance and reacting with surrounding molecular H_2O and O_2 to produce ROS. They produced a piezoelectric material containing gold nanoparticles in barium titanate nanocubes (Au@BTO NCs). It is well known that BTO has good electromechanical conversion and high voltage electrical coefficients, while the Schottky junction formed by chemically reducing Au NPs to the BTO surface can promote the separation and migration of electron-hole pairs, which in turn induces ROS generation [111]. Subsequent experiments by the researchers have confirmed that under the same US irradiation conditions (1.5 W/cm^2, 1 MHz), Au@BTO NCs have a higher •OH production capacity than BTO NCs. In *in vivo* experiments, the antibacterial efficiency reached 99.23% against *E. coli* and 99.94% against *S. aureus* after 4 min of irradiation with Au@BTO NCs. The antibacterial ability was also evaluated *in vitro* using a mouse model, and the results showed the best of *S. aureus* infected wound healing in the Au@BTO + US group.

5.2. Treatment for infected oral diseases

The oral cavity is a complex microbial environment with over 25,000 species of bacteria colonizing it. Under normal conditions, microorganisms live and multiply as biofilms on the teeth or mucous membranes and maintain a dynamic balance. When the immunity of the host is low, the environment of the oral cavity will change, allowing certain bacteria to become dominant and the balance between microorganisms to be disturbed, causing a range of oral diseases [112,113]. Due to the peculiarities of oral tissue structure and the development of resistance to conventional antibiotics, the search for a noninvasive, nonresistant and highly penetrating agent has become an alternative therapy to treat oral infectious diseases. Several recent reports suggest that aSDT is a treatment for oral infectious diseases [114,115]. In addition, the use of aSDT as a topical treatment, rather than systemic antibiotic treatment, can significantly reduce the associated side effects [116,117]. Since the application of SDT for antibacterial purposes, some scholars have made

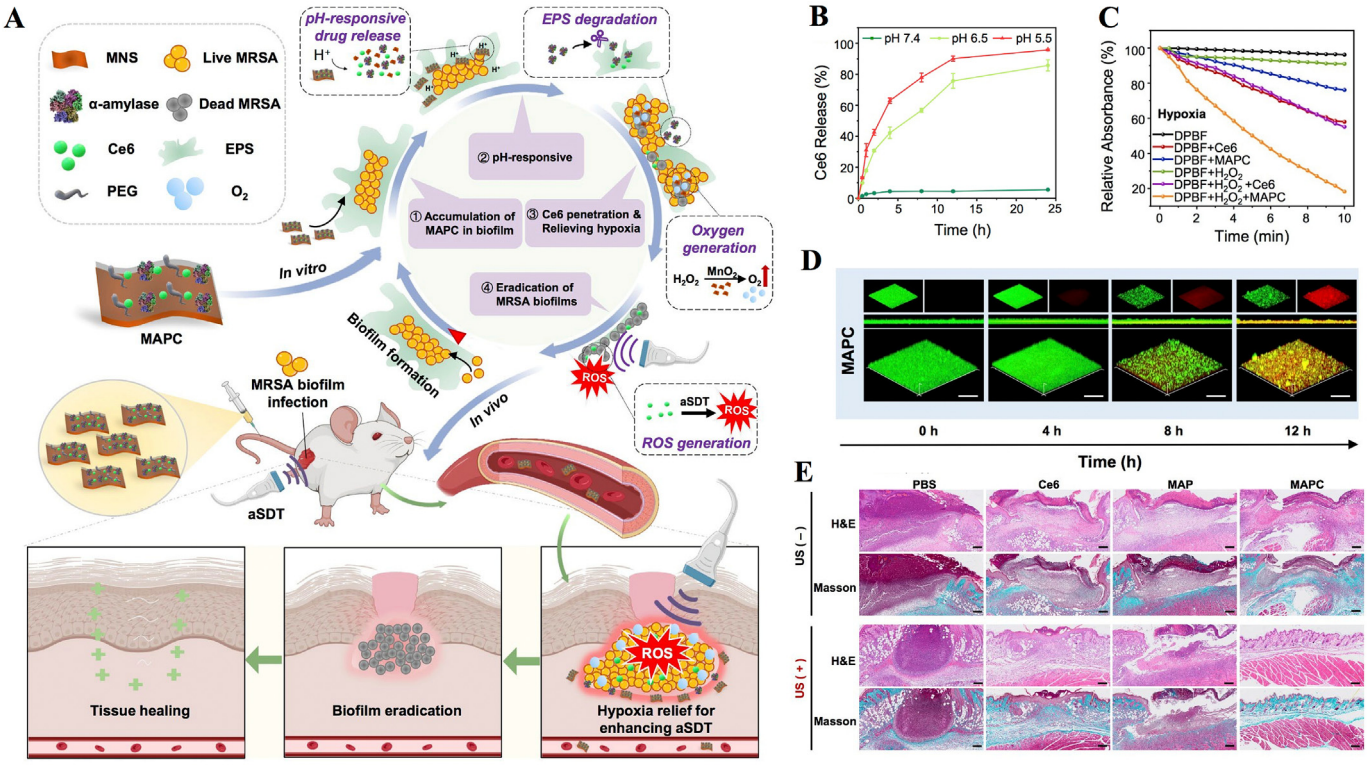

Fig. 3. Biofilm microenvironment response nanosonosensitizers synergistically degrade biofilm structure and relieve hypoxia for efficient aSDT. (A) Illustration of degradation of the biofilm structure by using a MAPC nanoplatform to enhance the biofilm eradication efficiency of aSDT. (B) Ce6 released from MAPC in PBS at acidic pH. (C) Singlet oxygen generation efficiency of nanosonosensitizers under US stimulation. (D) 3D CLSM images of MAPC after incubation with MRSA biofilms for different times. (E) H&E and Masson's trichrome staining images of the infected mouse tissues after aSDT [109]. Copyright©2022 Elsevier B·V.

significant achievements in the treatment of inflammatory oral infections such as caries, pulpitis, oral candidiasis and peri-implantitis.

Dental caries is a chronic process caused by the presence and interaction of microorganisms, a high carbohydrate diet and the host. The most common cause of dental caries is infection by *Streptococcus pyogenes*, a gram-positive, facultative anaerobic microorganism [118]. Pourhajibagher et al. synthesized nanomicelle curcumin (NM@Cur) as a sonosensitizer, and it was found that NM@Cur can inhibit *Streptococcus pyogenes* by aSDT (US parameters 1.56 W/cm^2, 1 MHz, 1 min) and increase anti-caries activity. Cur is a natural sonosensitizer with antioxidant, anti-inflammatory and antibacterial capabilities. However, because Cur is unstable in body fluids, hydrophobic, rapidly metabolized and cleared by the system, it is often encapsulated in nanoparticles to prevent degradation. In the experiments, they encapsulated Cur and successfully completed *in vitro* antibacterial experiments. Additionally, they found that NM@Cur was less cytotoxic to vascular endothelial cells and had higher cellular uptake and ROS production than the control group [62]. Pulpitis and periapical infection are treated by removing the infected pulp tissue and microorganisms with root canal therapy. However, the complexity of the anatomy of the root canal system makes it difficult to precisely reach the infected area with instruments, and plaque biofilms are difficult to eradicate, so the effectiveness of the irrigation agent becomes vital for the elimination and prevention of root canal infections. Guo et al. reported a Fenton reaction-enhanced SDT platform, which was fabricated for root canal disinfection (Fig. 4A) [60]. Mesoporous silica nanoparticles (MSNs) were first synthesized, grafted with an amino group and then conjugated with the sonosensitizer protoporphyrin IX (PpIX). Next, the iron ions were anchored (M@P–Fe) to initiate the Fenton reaction. US-activated (1 MHz, 0.5 W/cm^2, 3 min) PpIX and iron-mediated H_2O_2-generated Fenton reactions induce the formation of ROS. The results show that the platform can effectively eradicate root canal biofilms *in situ* (Fig. 4B).

5.3. Treatment for bone infections

Osteomyelitis is caused by microbial infection and accompanied by bone destruction, which often occurs after trauma, bone surgery or joint replacement [119]. MRSA is the most common causative agent of osteomyelitis, and can cause bone destruction at the infection site by secreting toxins, inducing osteoblast apoptosis and activating osteoclast formation [120]. Successful treatment of osteomyelitis depends on the rate and extent of penetration of antibiotics in the bone tissue [121]. However, osteomyelitis is a persistent infection and is located deep in the bone tissue, so antibiotic treatment often fails to achieve satisfactory results [122]. Due to high penetration and efficiency, aSDT is a promising approach to treat osteomyelitis.

Yu et al. reported a multifunctional nanoplatform for the treatment of MRSA-infected osteomyelitis. In brief, they synthesized a US-activated single-atom catalyst that consists of an Au nanorod-actuated single-atom-doped porphyrin metal-organic framework (HNTM-Pt@Au) and red cell membrane (RBC). This platform demonstrated unique advantages: the ultrasonic catalytic activity of the porphyrin-based sonosensitizer was enhanced in the presence of a single metal atom, while the RBC covering made RBC-HNTM-Pt@Au more biocompatible (Fig. 5A–D) [58]. It is worth mentioning that RBC-HNTM-Pt@Au can be directionally activated by US (1 MHz, 1.5 W/cm^2, 50% cycle, 15 min), followed by slow and continuous neutralization of the secreted toxin. Experiments in a rat model showed that treatment with US and RBC-HNTM-Pt@Au was effective in treating MRSA-infected osteomyelitis and prevented bone destruction. Several inflammatory indicators, such as the degree of

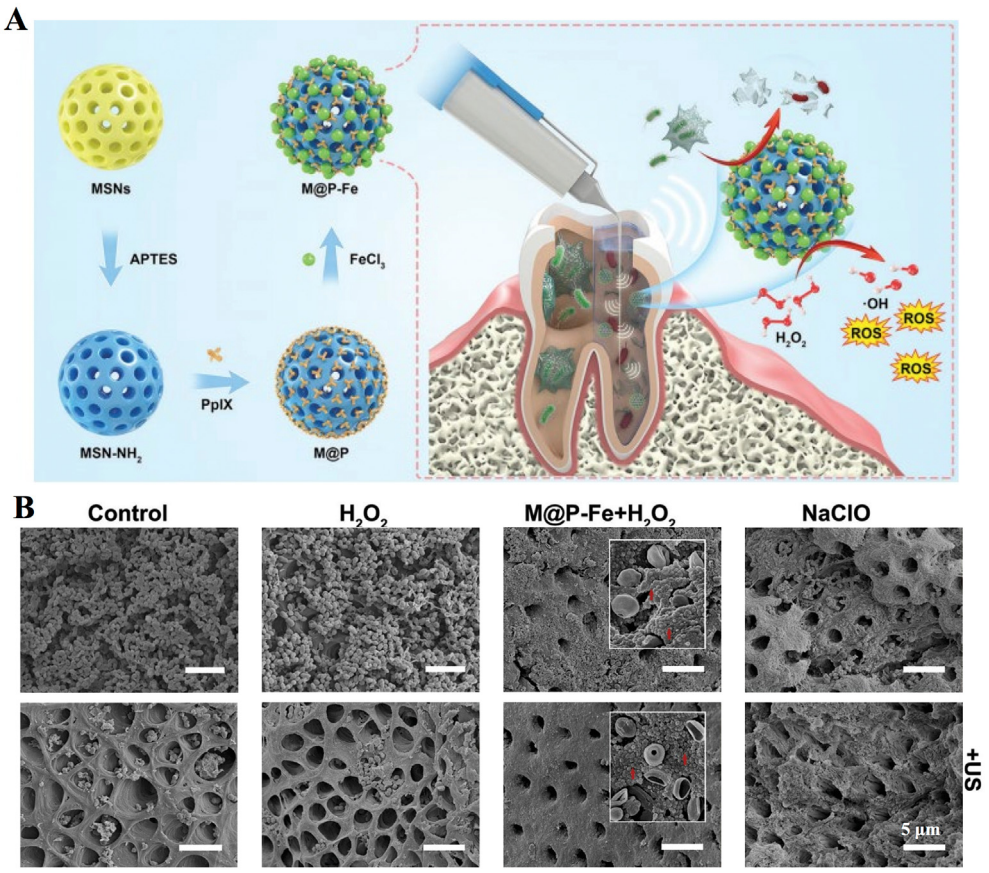

Fig. 4. Nanosonosensitizer-mediated aSDT for root canal disinfection. (A) Illustration of the synthesis and antibacterial mechanism of the nanosonosensitizers. (B) Representative SEM images of *E. faecalis* biofilms grown on a dentin root canal wall after different treatments [60]. Copyright © 2021, Royal Society of Chemistry.

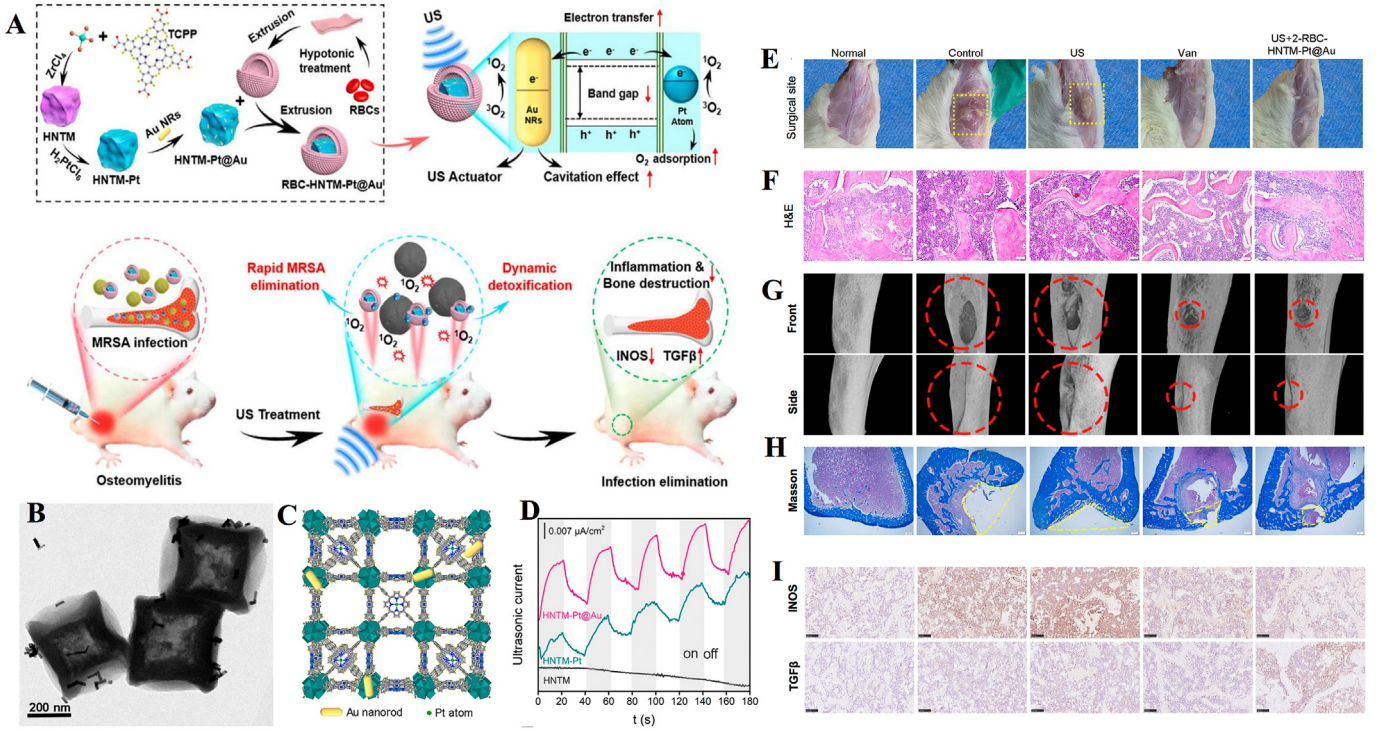

Fig. 5. Application of nanosonosensitizers in the treatment of osteomyelitis through efficient aSDT. (A) Synthesis of RBC-HNTM-Pt@Au and sonocatalytic mechanism for the treatment of osteomyelitis. (B) TEM images of HNTM-Pt@Au. (C) 3D structure of HNTM-Pt@Au. (D) Ultrasonic current test of different nanosonosensitizers. *In vivo* antibacterial performance. (E) Surgical site images, (F) H&E staining, (G) micro-CT images of tibial defects and (H) Masson staining images in infected bone tissues of rat models after 4 weeks of treatment. (I) Immunohistochemical staining of iNOS and TGFβ at week 2 of treatment [58]. Copyright©2021, American Chemical Society.

muscle tissue ulceration, infiltration of inflammatory cells, changes in the body weight of rats, and even the immune microenvironment and the area of bone defects at the site of infection were significantly improved compared to the control group (Fig. 5E–H). This study facilitates the process of *in situ*, rapid antimicrobial treatment of osteomyelitis, while providing a new idea for the development of a single-atom sonocatalyst.

Feng et al. constructed a piezoelectrically enhanced nanosonosensitizer to combat osteomyelitis infection (Fig. 6). These nanosonosensitizers (RBC-HNTM-MoS_2) were prepared by electrostatically interacting MoS_2 nanosheets modified on the surface of HNTM and decorated with RBC membranes [123]. Among these components, MoS_2 nanosheets have an excellent piezoelectric effect, and RBC membranes can improve biocompatibility in bone marrow. Under US irradiation (1.5 W/cm^2, 1.0 MHz, 15 min), RBC-HNTM-MoS_2 achieved an antibacterial efficiency of 90.5% against MARS *in vitro* and showed good therapeutic efficacy in the treatment of osteomyelitis infection *in vivo*. To explore the antimicrobial mechanism of nanosonosensitizer-mediated aSDT, the investigators performed a metabonomics study and found a significant increase in tryptophan metabolites in the HNTM-MoS_2+US group. This phenomenon was attributed to the production of more ROS oxidized tryptophan and induced a stronger oxidative stress response. In addition, elevated hypoxanthine and cyclic guanosine indicated accelerated nucleotide turnover following treatment, leading to higher levels of DNA damage. Reduced biosynthesis of pantothenate and CoA suggested interference with bacterial membrane function and cellular respiration.

In confrontation with the treatment of bacterial infections of bone defects, Lei et al. constructed a model of sulfur-containing oxygen-deficient BTO (SDBTO-1) using the piezoelectric properties of the system. Under 1.5 W/cm^2 US irradiation, a strong piezoelectric field continuously separates electron-hole pairs, leading to a redox reaction to produce ROS. The combined application of SDBTO-1 with US not only achieved an antibacterial effect of 97.12% against *S. aureus* but also contributed to bone differentiation [124]. The above examples of successful applications of piezoelectric nanocomposites in combination with US provide guidance for the development of new nanosonosensitizers, where the exploration of antibacterial mechanisms also reveals the way in which piezoelectric composites can be used in antibacterial applications.

5.4. Treatment for myositis

Myositis is defined as an acute intramuscular bacterial infection that is neither secondary to a continuous infection of soft tissue or bone nor due to penetrating trauma. The infection is the result of blood-borne transmission and is always caused by *S. aureus*. The common treatment for myositis is urgent and thorough surgical debridement and antibiotic treatment against *S. aureus* [125,126]. With the misuse of antibiotics, drug resistance is affected, and gradually, the effectiveness of treatment is not guaranteed.

Sun et al. modified Pd@Pt nanoplates with the organic sonosensitizer meso-tetra (4-carboxyphenyl) porphin (T790) *via* a polyethylene glycol (PEG) linker to acquire a Pd@Pt-T790 nanoplatform (Fig. 7A and B) [59]. Pd@Pt-T790 upon US irradiation (1 MHz, 0.97 W/cm^2, 50% cycle, 8 min) can increase the interaction of H_2O_2 with Pd@Pt to produce more O_2 (Fig. 7C). Moreover, wrinkled and lysed cell walls were observed in the group treated with Pd@Pt-T790-mediated aSDT (Fig. 7D). In addition, sustainable and strong oxyhemoglobin signals could still be observed after Pd@Pt-T790-mediated aSDT, and the blood oxygen level was much higher than that of other treatment groups on day 14 (Fig. 7E). The representative MRI photographs showed that the treatment in all control groups failed to eradicate MRSA-induced myositis with an obvious abscess cavity. In contrast, there was complete clearance of muscular lesions in mice with Pd@Pt-T790 + US treatment (Fig. 7F). H&E images showed that the muscle biopsy section had completely normal morphology in the Pd@Pt-T790 + US treated group (Fig. 7G). Thus, it was found to be significantly effective in eradicating

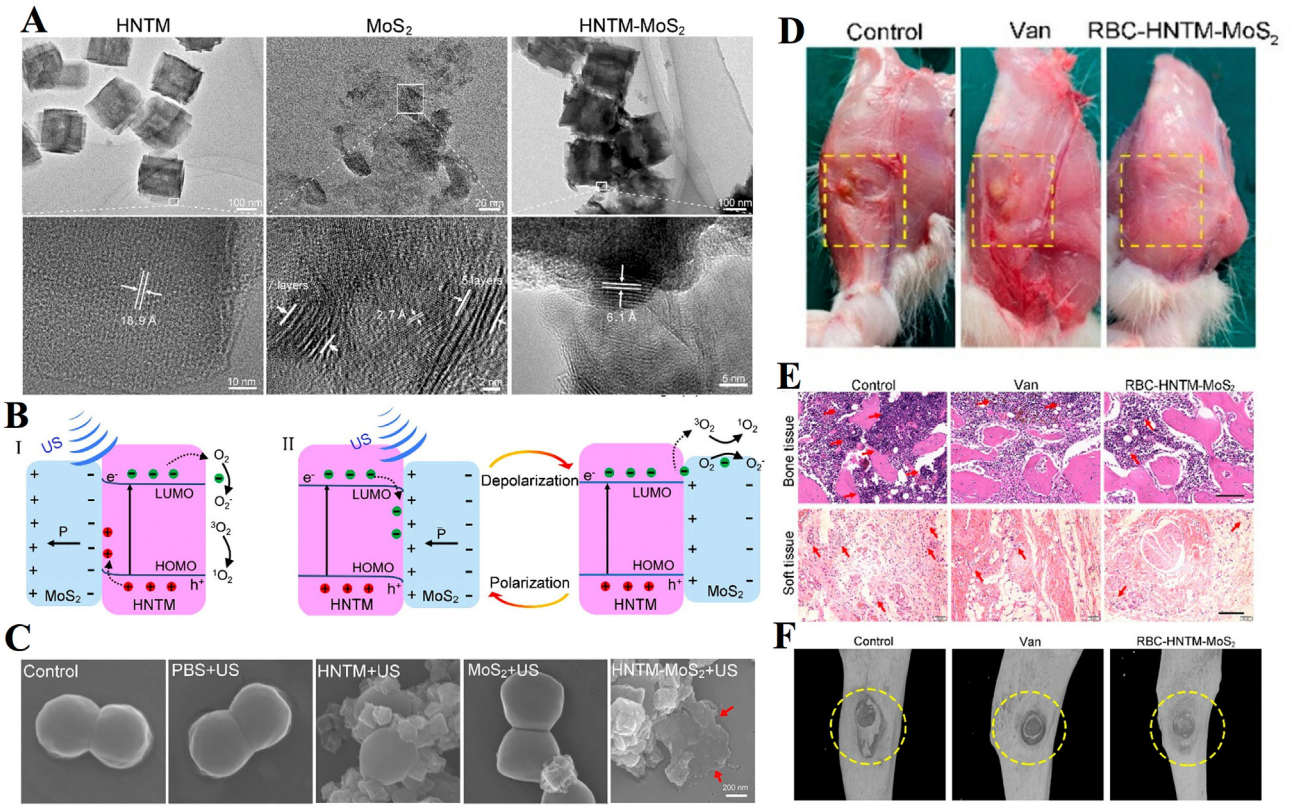

Fig. 6. Piezo-Augmented Sonosensitizer for aSDT. (A) HRTEM images of HNTM, MoS_2 nanosheets, and HNTM-MoS_2. (B) US-induced piezoelectric-enhanced sonocatalytic mechanism. (C) SEM images of MRSA in different groups. (D) Wound images of infected sites. (E) H&E staining of the infected bone and soft tissue. (F) Micro-CT of the infected legs in different groups [123]. Copyright©2022, American Chemical Society.

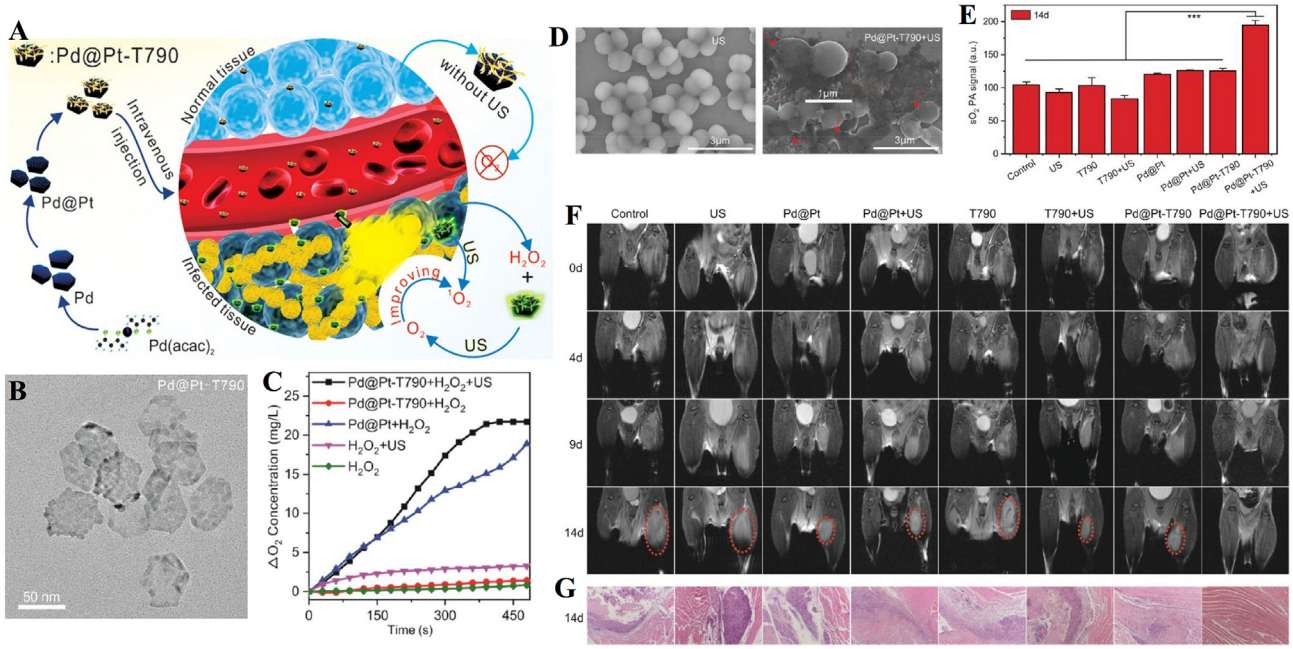

Fig. 7. US-switchable nanozyme mediated aSDT for myositis. (A) Schematic illustration of the synthesis procedure of the Pd@Pt-T790 nanoplatform and its US-switchable nanozyme catalytic oxygen-generation-enhanced aSDT. (D) Representative SEM images of MRSA incubated with Pd@Pt-T790 + US. (E) Comparison of the degree of sO_2 from the PAI at 14 days for different treated myositis groups. (F) Representative magnetic resonance and (G) histological images of MRSA myositis on day 14 after treatment [59]. Copyright©2020, American Chemical Society.

MRSA-induced deep myositis. In addition, Huang et al. developed nanosonosensitizers based on PLGA nanoparticles and loaded them with IR780 to monitor aSDT in MRSA myositis by US irradiation (1 MHz, 2 W/cm^2, 50% cycle, 30 s on and 30 s off for four on/off cycles). In this

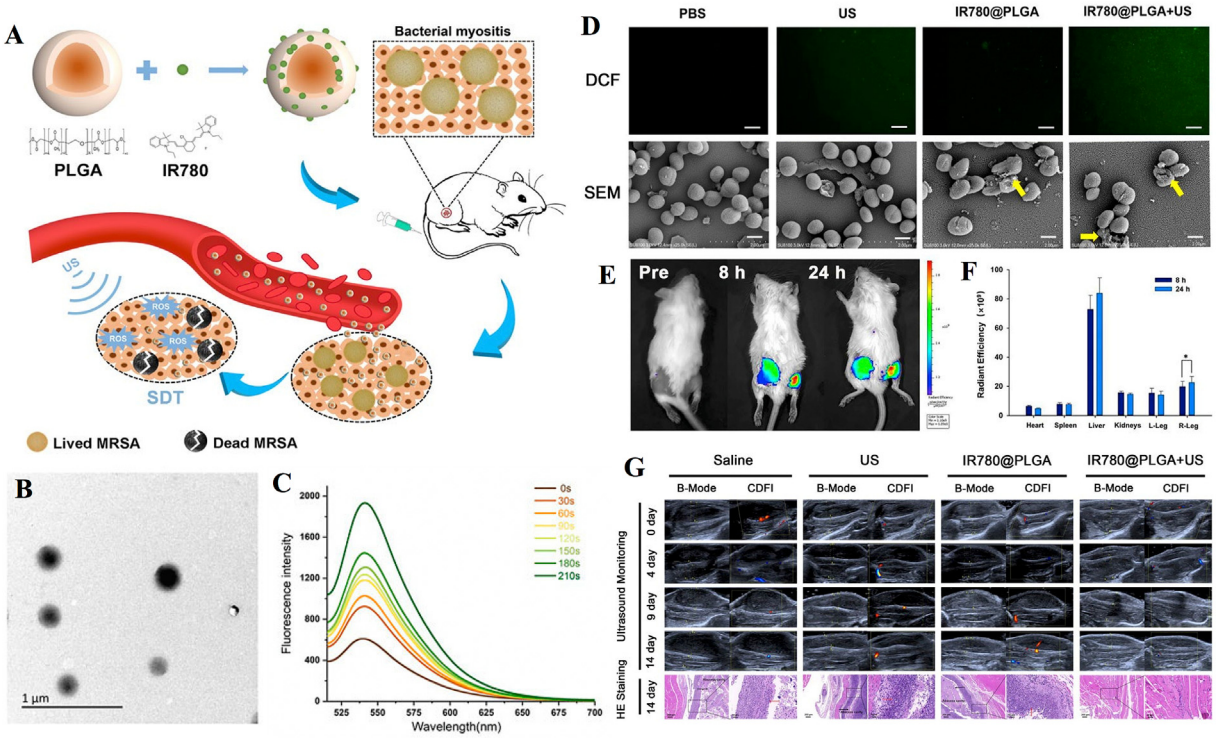

Fig. 8. IR780@PLGA nanoparticle-mediated aSDT for myositis. (A) Schematic illustration of the sonotherapeutic IR780@PLGA nanoparticles for combating multidrug-resistant bacterial infections. (B) TEM image of IR780@PLGA nanoparticles. (C) Time-dependent $^1O_2$ generation of IR780@PLGA nanoparticles with US irradiation (1 MHz, 2.0 W/cm^2). (D) Fluorescent images of DCF-stained $^1O_2$ generation by bacteria and SEM images of the bacterial biofilm in different groups. (E) Time-lapse NIR fluorescence images of MRSA-infected mice *in vivo* after injection of IR780@PLGA nanoparticles. (F) Averaged *ex vivo* NIR fluorescence intensities. (G) Representative US and histological images of MRSA-infected mice in different groups [61]. Copyright@2022, Huang B et al.

study, shell-core structured IR780@PLGA nanoparticles were designed as PLGA with a polymer shell loaded with the sonosensitizer IR780 (Fig. 8). *In vitro* and *in vivo* results confirmed that IR780@PLGA nanoparticles in combination with US possess efficient antimicrobial therapy [61]. The successful preparation and application of these two nanoplatforms reveal the promising antimicrobial effects of nanosonosensitizers in aSDT against bacterial myositis. Additionally, for the treatment of bacterial myositis, Pang et al. developed a bacterial-specific labeling and visualization of aSDT. This platform (MLP18) consists of maltose hexose-modified cholesterol and bacterially reactive lipids for the precise delivery of purines18. The results showed that MLP18-mediated aSDT (US parameters 1 MHz, 0.97 W/cm^2, 5 min) can successfully eliminate infection and abscesses in mice with bacterial myositis [52].

6. Combination of aSDT with other therapies

As discussed above, many sonosensitizers are utilized for their remarkable aSDT-related sterilization capabilities. aSDT is widely used due to its non-invasive nature and excellent tissue penetration, resulting in impressive sterilization results. Unfortunately, some studies have found that aSDT alone cannot completely kill bacteria in specific contexts. In the face of these challenges, researchers have combined aSDT with other treatments, such as PDT, PTT, antibacterial drugs, immunotherapy and chemodynamic therapy (CDT), to achieve synergistic antibacterial effects.

6.1. Combination of aSDT with PDT

Antimicrobial PDT produces cytotoxic singlet oxygen and free radicals by the interaction of photosensitizers with visible light or ultraviolet light to induce harmful effects on microorganisms [127]. However, the application of PDT in clinical infectious diseases is limited to the area that light can reach, namely between a few millimeters and centimeters, which is not sufficient for deep infectious diseases. To compensate for the shortcomings of PDT, the combined application of PDT and SDT (PSDT) is gradually being explored for its unique advantages. Xu et al. reported the exploitation of yolk-structured multifunctional upconversion nanoparticles (UCNP@SiO_2-RB/HMME) to effectively kill antibiotic-resistant bacteria [128]. *In vitro* experiments have shown that UCNP@SiO_2-RB/HMME is more effective against both MARS and *E. coli* in PSDT than SDT or PDT alone. Recently, Pourhajibagher et al. synthesized curcumin-nisin-based poly (L-lactic acid) nanoparticles (Cur-NisNps) and evaluated their antibiofilm and wound healing activities in mice with established *A. baumannii* infections [55]. In his conclusion, Cur-NisNp-mediated PSDT might be a promising complementary approach to treat burn wound infections (Fig. 9). In this study, US was used at a frequency of 1 MHz with a pulse repetition rate of 100 Hz. The light wavelength was 435 ± 10 nm and the output intensity was 1.0–1.4 W/cm^2. *In vitro* and *in vivo* experiments demonstrated that Cur-NisNp-mediated PSDT altered gene expression in bacterial pathogenesis, further inhibited biofilm growth of *A. baumannii* and promoted wound healing by accelerating skin re-epithelialization.

Peri-implantitis is an inflammatory disease of the oral cavity with a bacterially dominant etiology. Treatment for peri-implantitis aims to reduce the bacteria loading in the peri-implant pocket and to clean the surface of the implant to promote osseointegration [129]. Topical application of antimicrobial solutions such as chlorhexidine and tetracycline, mechanical decontamination and the use of lasers or other alternative light sources as physical methods are all common methods of treating peri-implantitis. After synthesizing chitosan nanoparticle-indocyanine green (CNPs-ICG) as a photosonosensitizer, Pourhajibagher et al. constructed a mature biofilm model of synergistic polymicrobial action of surrounding pathogens on the surface of titanium implants [56]. The researchers used both PDT (diode laser irradiation at a wavelength of 810 nm for 1 min with an energy density of 31.2 J/cm^2)

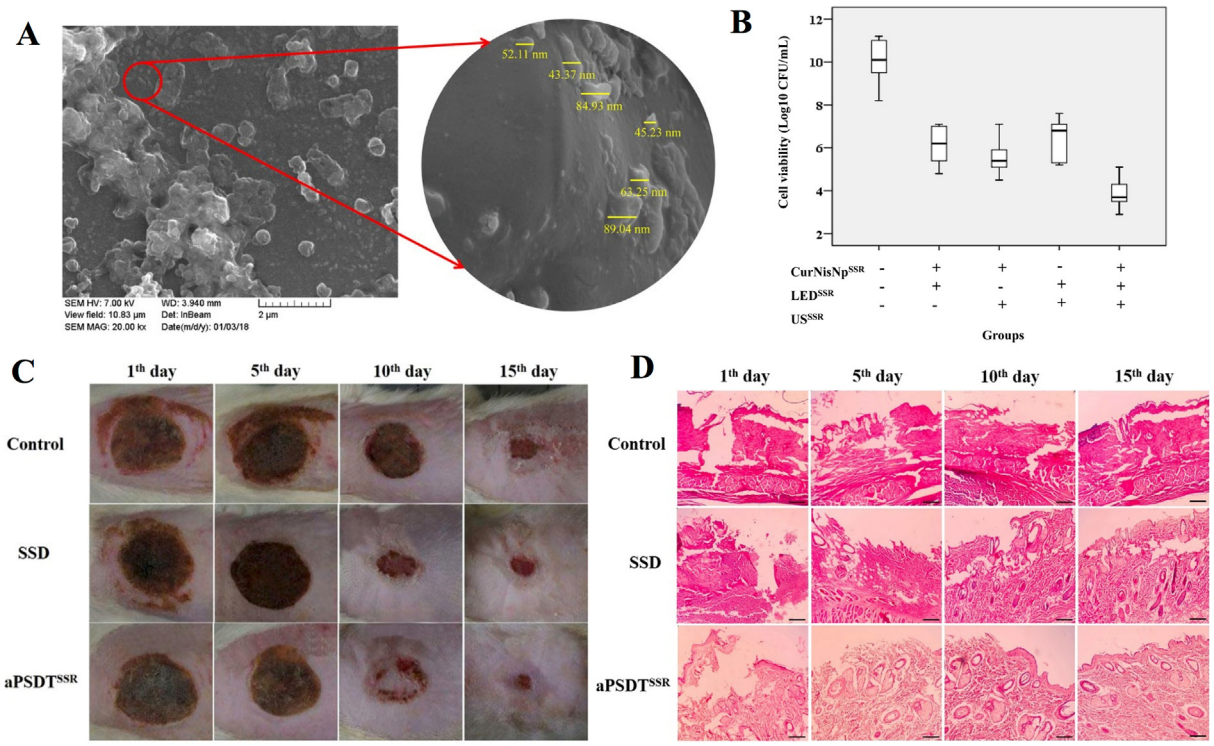

Fig. 9. Nanosonosensitizer-mediated PSDT to treat burn wound infections. (A) Field emission scanning electron microscopy (FESEM) image of nanosonosensitizers (Cur-NisNp). (B) The antimicrobial effects of Cur-NisNp under LED irradiation, US irradiation, and their combination against *A. baumannii*. (C) Wound healing process in different treatment groups. (D) H&E images of burn wound skin tissues [55]. Copyright©2022, Springer Nature.

and SDT (US with an intensity of 1.56 W/cm^2 for 1 min at a frequency of 1 MHz) to inhibit the biofilm of pathogenic bacteria around the surface of the titanium implants. As control groups, the results of *in vitro* antimicrobial assays demonstrated that combined treatment with PSDT was more effective than treatment with PDT or SDT alone in reducing the number of peripheral pathogenic bacteria, which highlights the potential of PSDT/CNPs-ICG for synergistic polymicrobial decontamination on implant surfaces.

6.2. Combination of aSDT with PTT

PTT increases the local temperature through non-invasive light exposure, ultimately destroying the integrity of the bacteria [130]. The mechanism of PTT is to kill the protected bacteria by disrupting the structure of biofilms by inactivating their inherent bioactive substrates, such as nucleic acids and proteins, through high temperatures [131,132]. However, the efficiency of photothermal conversion is greatly reduced due to the inevitable light scattering and absorption effects. Unfortunately, the higher sterilization temperatures leave normal cells and tissues damaged [132,133]. The synergistic treatments of aSDT and PTT have received increasing and widespread attention in recent years. Bi et al. used silver oxide nanoparticles (Ag_2O_2 NPs) as H_2O_2 and O_2 generators to induce oxidative stress reactions with the simultaneous release of silver ions (Ag^+). Based on the property that Ag_2O_2 NPs can be activated by US and NIR, investigators used Ag_2O_2 NPs in combination with aSDT and PTT, and both *in vitro* and *in vivo* experiments showed excellent anti-free bacterial and anti-biofilm activity [50].

One of the reasons for implant failure is periprosthetic infection [134]. The presence of bone implants leads to an increased risk of infection due to the creation of an immunodeficient area in the vicinity of the implant. In the implantation area, the ability of the host to clear contaminated bacteria may be impaired, which may lead to the formation of biofilms on the surface of the biological material [135]. When a biofilm has formed, treatment with antibiotics and the immune system is not sufficient, and sometimes a second operation is required to replace the infected implant [136]. Most studies have found that *in vivo* models, conventional strategies such as regulation of the immune system and the use of systemic antibiotics do not eliminate biofilms [137]. To address this problem, combined aSDT and PTT is a nonsurgical, noninvasive treatment for biofilm infections. Su et al. developed an S-doped Ti implant (Ti–S–TiO_{2-x}) to improve the efficiency of PTT and SDT (Fig. 10A). The titanium implant was heated in a sulfur and argon atmosphere to achieve an oxygen-deficient S-doped TiO_2 layer. Along with titanium being inherently biosafe and biocompatible, blending with nanosonosensitizers improved NIR light absorption and electron-hole separation efficiency. In both *in vitro* and *in vivo* experiments, the platform showed efficient antimicrobial performance in the presence of exogenous stimulation (US + 808 nm laser) and without the use of an external antimicrobial coating (Fig. 10B and C). *In vitro* experiments showed that the synthesis and application of Ti–S–TiO_{2-x} achieved 99.995% inhibition efficiency against *S. aureus* under NIR light (808 nm, 0.35 W/cm^2) and US treatment (1 MHz, 1.5 W/cm^2, 50% cycle) for 15 min. However, in the single PTT or SDT treatment group, despite the much higher antibacterial efficiency of Ti–S–TiO_{2-x} than in the Ti group, it was not effective in killing *S. aureus* due to its mild heating (50 °C) or limited ROS production. They then investigated the antibacterial performance of implants against the anaerobic bacteria *Porphyromanus gingivalis* (*P. gingivalis*). The results showed an antibacterial efficiency of 99.61% after US and photothermal treatment, which indicates that the combined treatment also has highly effective antibacterial properties against anaerobic bacteria. In addition, reduced infection and improved osseointegration were observed in a rat model of bone infection. Bone screws were covered with bacteria and then implanted in the tibia of rats. These S-treated bone screws covered by bacteria achieved an antimicrobial efficiency of 99.26%, demonstrating that clinically used implants can also achieve efficient antimicrobial properties *in vivo* (Fig. 10D–F).

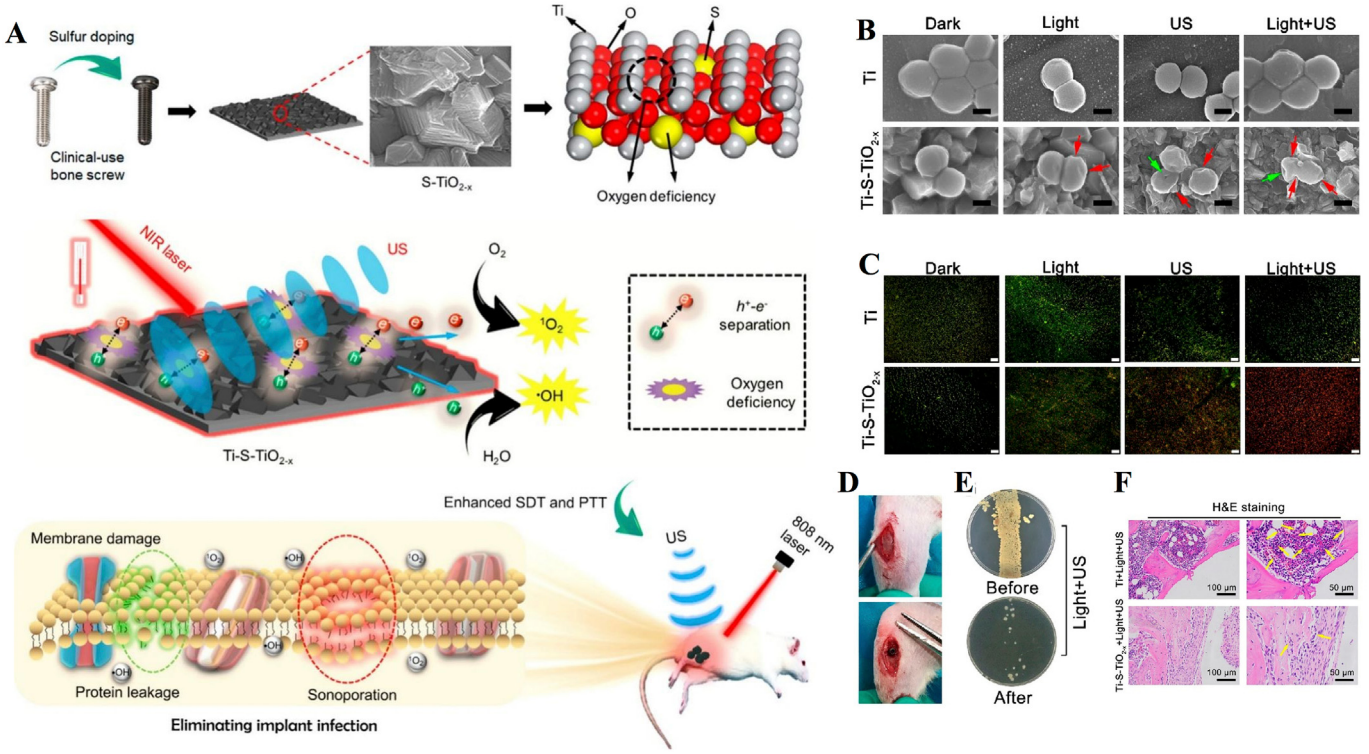

Fig. 10. Combination of aSDT with PTT for infected bone implants. (A) Schematic illustration shows that the sulfur-doped clinically used bone screw has enhanced sonocatalytic-photothermal ability by producing oxygen deficiency and shows efficient bone infection therapy. (B) SEM images and (C) fluorescence images of *S. aureus* in different treatment groups. (D) Implant site and (E) antibacterial performance of the S-treated bone screws. (F) H&E staining of the bone tissue around the implants [49]. Copyright©2020, American Chemical Society.

6.3. Combination of aSDT with antibacterial drugs

In recent years, with the rapid development of drug delivery technology, the use of drug-loaded nanoparticles for antibacterial applications has shown great potential [138]. Due to the inherent antibacterial properties of nanoparticles and their ability to act as drug carriers, they can protect against a variety of pathogenic microorganisms at low concentrations, while being unlikely to cause the emergence of drug resistance. It has been reported that the use of US stimulation can enhance drug delivery; thus, researchers have attempted to combine nanosonosensitizers with antibiotics in the treatment of specific pathogens. Yang et al. investigated the synergistic antifungal effects of the combination of AmB-containing PLGA nanoparticles and US irradiation for the treatment of *C. albicans* [54]. After synthesizing AmB nanoparticles, the researchers first tested the activity of *C. albicans* with SDT alone and found that with US parameters of 0.3 W/cm^2 and 15 min, *C. albicans* was active but it showed damage to the cell wall barrier and increased cell permeability. It was then decided to use this parameter as an effective parameter for the combined application. After the combined effect, the survival of *C. albicans* was significantly lower (91% ± 0.12%) after exposure to US and treatment with AmB-NPs compared to the control group. It is noteworthy that the survival rate in the combined treatment group was significantly lower than for AmB alone or US combined with free AmB. Although the pathogen targeted in this experiment was a fungus, with the above practice as a basis, the combination of US and drug-loaded nanoparticles can be considered a promising anti-infective treatment strategy.

6.4. Combination of SDT with immunotherapy

Bacteria produce virulence factors after destroying the host or evading and circumventing the host immune system. Antiviral treatment approaches attempt to interfere with these factors to treat the infection. This treatment counteracts immunosuppression and protects the innate immune defenses from toxic attacks [139]. Dickey et al. suggested that empirical treatment may require the use of antivirals in combination with other antimicrobial drugs to increase therapeutic coverage of bacteria. In addition, combination therapy may also be necessary for pathogens that produce several virulence factors to overcome the possible crossover effects between these factors [140]. Therefore, combined aSDT with antivirulence-mediated immunotherapy may provide an idea to cure bacterial infections. Based on previous findings that cell membrane nanovesicles can exhibit a variety of application-specific peptide or protein ligand properties under suitable treatment, Pang et al. developed novel MAb-piloting nanovesicles (ANVs) through genetic membrane engineering technology for combined aSDT and antivirulence passive immunotherapy cascade [53]. These ANVs target two key pathogenic mechanisms of bacterial infection: attacking bacteria and inhibiting toxin secretion (Fig. 11). Upon US activation, the nanosonosensitizers efficiently produce ROS to kill bacteria and assist in virulence clearance by antibodies. In addition to capturing both bacteria and associated virulence, these ANVs also allow precise optical diagnosis of MRSA infection due to the highly specific antibody-ligand interaction and inherent luminescent features of nanosonosensitizers.

6.5. Combination of SDT with CDT

Chemodynamic therapy (CDT) stimulates the formation of highly toxic •OH *via* Fenton or Fenton-like reactions with H_2O_2 [25]. Due to its low side effects, low cost of treatment, high broad-spectrum antibacterial activity and susceptibility to multidrug resistance, CDT has played an irreplaceable role in the successful application of biomedicine. CDT has been used in combination with other therapies such as SDT, PTT, chemotherapy, and immunotherapy to achieve enhanced anticancer

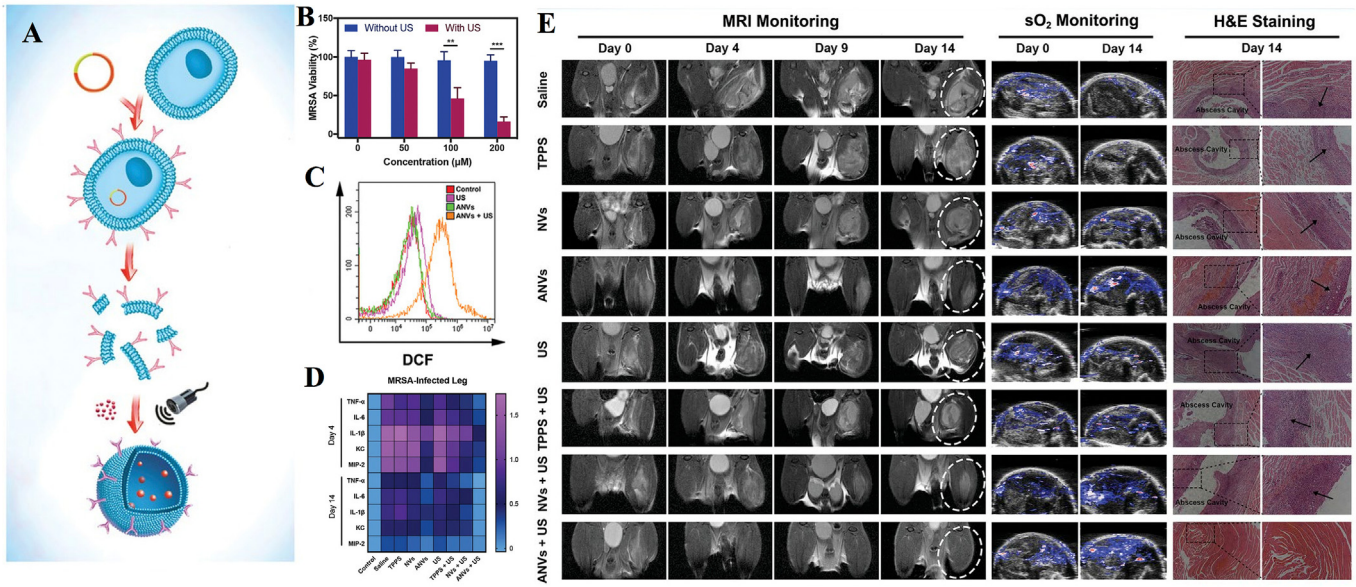

Fig. 11. Combination of SDT with immunotherapy for MRSA myositis. (A) Schematic illustration of the budding process of ANVs nanocapturers from antibody-overexpressing cells. (B) Dependence of the bacterial survival fraction on the concentration of ANVs under ultrasound irradiation. (C) Measurement of ROS levels in MRSA using flow cytometry with DCFH-DA staining. (D) MRSA-infected leg from mice at Day 4 and Day 14. (E) Representative magnetic resonance images, PA images of oxyhemoglobin saturation, and histological images of MRSA-infected mice [53]. Copyright©2019 WILEY-VCH Verlag GmbH & Co. KGaA, Weinheim.

effects. There are also studies extending the combined use of CDT to the antimicrobial field. Liang et al. developed a CuO_2/TiO_2 heterostructure consisting of CuO_2 nanoclusters and oxygen vacancy-rich porous titanium oxide ($OVTiO_2$) nanosheets, and subsequently incorporated the complex into microneedles to enhance the effects of sono-chemodynamic and thermal antibacterial therapy [141]. In *in vitro* experiments, the number of MRSA and *P. aeruginosa* colonies in the CuO_2/TiO_2+US group was reduced by 7.30 and 7.35 orders of magnitude, respectively, after 5 min of US radiation (1.0 W/cm^2, 1 MHz), with an inhibition rate >99.9999%. Satisfactory therapeutic results were obtained in a mouse model of skin wound infection after the incorporation of the composite material (CuO_2/TiO_2) into microneedles (CTMN). The results showed remarkable wound healing and reduced levels of inflammatory cytokines in the CTMN + US group (Fig. 12).

7. Conclusion and perspectives

Based on the findings described in this review, clinical translation becomes possible as the efficiency of aSDT is significantly enhanced with the expansion of exploration in nanomaterial-mediated sonosensitizers. Nanomaterial-mediated aSDT makes good use of the strong targeted expression and high permeability of nanomaterials while retaining the advantages of sonosensitizers to enhance acoustic effects. Beyond the study of natural nanoscale sonosensitizers, researchers have also achieved desirable antibacterial effects by combining nanomaterials with sonosensitizers through an encapsulated, conjugated route. To date, aSDT has been shown to be helpful in a number of clinical infection management areas, such as skin infections, oral infections, bone infections, and myositis.

The aSDT has shown unlimited potential as an emerging tool in antimicrobial therapy. However, due to uncertainties in the rationalization of various experimental studies, it still has a long way to go before it is actually used clinically, and this approach is still in its preliminary stages. To make them truly operable, future improvements are required in the following.

(1) Defined mechanisms

The mechanisms of SDT, let alone aSDT, have not been well researched, which has largely limited the development of aSDT. Only by describing its mechanism in all its aspects can we better control the antimicrobial effect from a physiological point of view.

(2) Standard US safety parameters

US with intensities below 3 W/cm^2 is defined as low-energy US, and US with frequencies below 1 MHz is defined as low-frequency US. Researchers usually conduct antibacterial experiments at low frequencies and low intensities of US, but the optimal parameters and safety parameters for US applications are rarely specified. A report proposed a method to inhibit the viability of *E. coli* by therapeutic US irradiation and found that the antibacterial effect varied at different doses of US irradiation (1 W/cm^2 and 3 W/cm^2), as demonstrated by a significant reduction in the viability of *E. coli* at higher US intensities (3 W/cm^2) [48]. It has been suggested that high frequency US leads mainly to a reduction in bacterial clumping, while low frequency US leads mainly to microbial inactivation [142]. Researchers still need to determine the most reasonable US parameters for different scenarios. In other words, the application of US parameters for various bacteria, sites of infection and modes of infection has not been explored in a mature manner, which largely limits the efficiency of aSDT. The link between US parameters and nanosonosensitizers has not yet been clearly explained and answered. Interestingly, differences in the parameters used by the researchers were found during the comparison of the antibacterial effect exerted by conventional sonosensitizers and nanosonosensitizers. A distinct example will be briefly described. A paper on HMME-mediated SDT of *P. gingivalis* with parameters of 3 W/cm^2, 1 MHz, and 10 min was applied in an *in vitro* antimicrobial experiment [143]. In another report on HMME-mediated SDT against *S. aureus*, it was shown that 95% of colonies were effectively killed under US parameters of 6 W/cm^2, 1 MHz and 30 min [144]. However, with appropriate nanotechnological modifications of HMME, satisfactory bactericidal effects were achieved for both *MARA* and *E. coli* at 2 W/cm^2 and 10 min of treatment with US parameters [64,128]. By analyzing and comparing the results of current experiments, it is easy to conclude that the use of nanotechnology has made it possible to achieve safe and effective antibacterial effects at lower frequencies and lower energies with US.

Although nanosonosensitizers have been developed, various acoustic

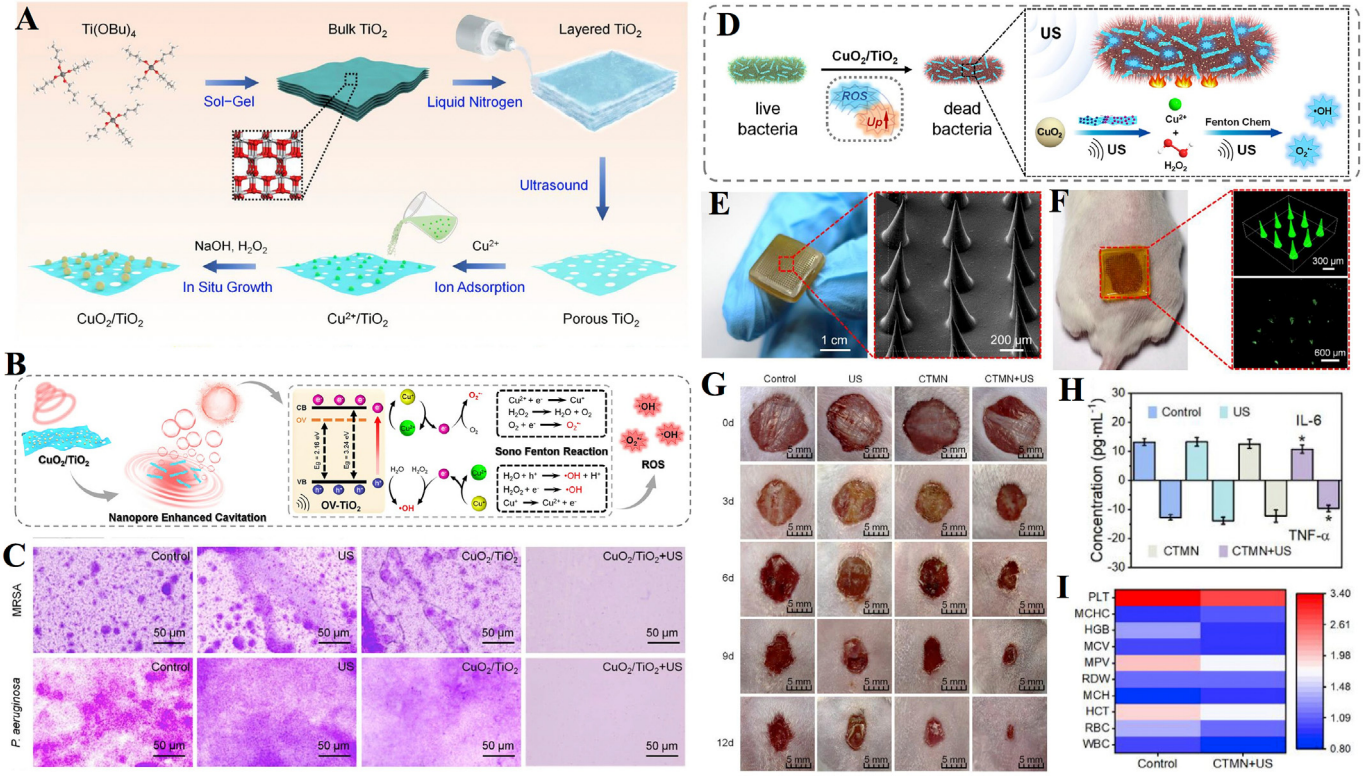

Fig. 12. Combination of SDT with CDT. (A) Schematic illustration of the synthetic route of CuO_2/TiO_2 nanostructures. (B) The sonodynamically enhanced ROS production mechanism of CuO_2/TiO_2. (C) Crystal violet staining images of MRSA and *P. aeruginosa* biofilms upon different treatments. (D) Illustration of the possible antibacterial mechanism of CuO_2/TiO_2. (E) Preparation and characterization of CTMN. (F) Topical application of FITC loaded CTMN on mouse dorsal skin. (G) Representative images of wounds infected with MRSA in different groups. (H) IL-6 and TNF-α levels in the sera of mice at the end of different treatments. (I) The blood test panel of mice after 12 days of treatment [141]. Copyright©2022 Acta Materialia Inc. Published by Elsevier Ltd. All rights reserved.

parameters and experimental settings make the quantification of these techniques ambiguous. It is difficult to give a clear definition of the US safety parameters. From this point of view, more detailed criteria to address specific models of inflammatory infection are needed. With the traditional range of 0.5–2.0 MHz, an intensity of 0.5–3.0 W/cm^2 and an irradiation time of 1–30 min, the parameters of US application are difficult to determine, and investigators need to take extra care in the dosage of US.

(3) Stimulus-responsive nanosonosensitizers

Sonosensitizers play a vital role in SDT, however, the question of how to effectively deliver them to the site of infection has not been resolved. Improving the targeting of nanosonosensitizers could be a direction for future research development. Thus, the development of stimulus-responsive nanosonosensitizers is particularly important. Some studies have introduced the simultaneous use of two or more nano-sonosensitizers and the codelivery of multiple sonosensitizers *via* a single nanocarrier, which has also been shown to improve the effect of aSDT.

(4) Preclinical studies in aSDT

The high heterogeneity and adaptability of the infection itself poses a great challenge for aSDT. Improving such novel antimicrobial therapies highly relies on increasing the susceptibility of bacteria to aSDT and breaking the cell-induced protective barrier of surviving cells under aSDT. In addition, the lack of suitable preclinical models of multidrug resistance and multibacterial infections is also a limitation that needs to be addressed. Although many researchers have applied their material models to different colony conditions to observe therapeutic effects, such studies are still mostly confined to *in vitro* and small animal models. Future research efforts should focus on translating the research to large animals and humans. Although, the aSDT is attracting increasing interest from researchers, it remains to be tested experimentally before transfer to clinical antimicrobial drug therapy.

(5) Hypoxia in infected areas

In conflict with the fact that bacterially infected areas often form a hypoxic environment, the process of SDT action requires the support of large amounts of oxygen, thus limiting the efficiency of SDT to some extent. With these challenges, modifications to the sonosensitizer, such as the use of oxygen production *in situ* in the microenvironment of the infected area, are required to solve the hypoxic dilemma.

(6) Biodegradable and biocompatible nanosonosensitizers

The ultimate goal of material development is clinical translation. When sonosensitizers are used in organisms, their good biodegradability and biocompatibility are prerequisites. Current studies have tended to focus on *in vivo* models, and *in vitro* experiments have been limited to animal models. Researchers have mainly focused on the acoustically sensitive effects of the materials and the antimicrobial effects in conjunction with US, while few studies have been conducted to analyze the metabolic pathways of their sonosensitizers. In the future, to reduce the side effects of residual sensitizers on the body, nanosonosensitizers with enhanced biodegradability and biocompatibility may have potential clinical applications. A number of bactericidal polymers containing intrinsically bactericidal components such as, phosphine groups, poly-anions, antimicrobial peptides (AMPs), quaternary ammonium

compounds (QACs) and antimicrobial enzymes (AMEs) have been used to investigate modification strategies [145]. They benefit from the abundance of functional groups on the polymers and can be structurally modified in different ways. Studies have reported that post-modification of polymers enhances their biocompatibility and cyclic stability, and even allows for specific recognition of bacteria. The modification of the polymer backbone can make the material functional in terms of stimulus responsiveness and degradability. Future researchers can focus on this hotspot and modify existing or recombinant nanosonosensitizers to advance the possibility of translating the materials into clinical applications.

Declaration of competing interest

The authors declare that they have no known competing financial interests or personal relationships that could have appeared to influence the work reported in this paper.

Data availability

No data was used for the research described in the article.

Acknowledgments

Financial support was provided by the National Natural Sciences Foundation of China (81571800), Key Project of Research, Development Plan of Jiangsu Province (BE2020629), Natural Science Foundation of Jiangsu Province (BK20200710), Development of Science and Technology of Nanjing (YKK19094), and “3456” Cultivation Program for Junior Talents of Nanjing Stomatological Hospital, Medical School of Nanjing University (0222R212). The authors also want to thank BioRender for providing drawing elements, which helped visualize our research.

References

[1] K. Hede, Antibiotic resistance: an infectious arms race, Nature 509 (7498) (2014) S2–S3.
[2] W.J. Xiu, et al., Recent development of nanomedicine for the treatment of bacterial biofilm infections, View 2 (1) (2021) 20200065.
[3] T.C. Porco, et al., When does overuse of antibiotics become a tragedy of the commons? PLoS One 7 (12) (2012), e46505.
[4] J.M. Blair, et al., Molecular mechanisms of antibiotic resistance, Nat. Rev. Microbiol. 13 (1) (2015) 42–51.
[5] F.F. Sperandio, Y.Y. Huang, M.R. Hamblin, Antimicrobial photodynamic therapy to kill Gram-negative bacteria, Recent Pat. Anti-Infect. Drug Discov. 8 (2) (2013) 108–120.
[6] A.S. da Fonseca, A.L. Mencalha, F. de Paoli, Antimicrobial photodynamic therapy against Acinetobacter baumannii, Photodiagnosis Photodyn. Ther. 35 (2021), 102430.
[7] L. Chambrone, H.L. Wang, G.E. Romanos, Antimicrobial photodynamic therapy for the treatment of periodontitis and peri-implantitis: an American Academy of Periodontology best evidence review, J. Periodontol. 89 (7) (2018) 783–803.
[8] S.P. Songca, Y. Adjei, Applications of antimicrobial photodynamic therapy against bacterial biofilms, Int. J. Mol. Sci. 23 (6) (2022) 3209.
[9] C. Cao, et al., POD Nanozyme optimized by charge separation engineering for light/pH activated bacteria catalytic/photodynamic therapy, Signal Transduct. Targeted Ther. 7 (1) (2022) 86.
[10] X. Lv, et al., Recent advances in pH-responsive nanomaterials for anti-infective therapy, J. Mater. Chem. B 8 (47) (2020) 10700–10711.
[11] D.L. Yang, et al., Orthogonal Aza-BODIPY-BODIPY dyad as heavy-atom free photosensitizer for photo-initiated antibacterial therapy, Journal of Innovative Optical Health, Sciences 15 (1) (2022) 2250004.
[12] A.P. Castano, P. Mroz, M.R. Hamblin, Photodynamic therapy and anti-tumour immunity, Nat. Rev. Cancer 6 (7) (2006) 535–545.
[13] T.J. Dougherty, et al., Photodynamic therapy, J. Natl. Cancer Inst. 90 (12) (1998) 889–905.
[14] E.J. Prażmo, R.A. Godlewska, A.B. Mielczarek, Effectiveness of repeated photodynamic therapy in the elimination of intracanal Enterococcus faecalis biofilm: an in vitro study, Laser Med. Sci. 32 (3) (2017) 655–661.
[15] X. Li, et al., Clinical development and potential of photothermal and photodynamic therapies for cancer, Nat. Rev. Clin. Oncol. 17 (11) (2020) 657–674.
[16] F. Cieplik, et al., Antimicrobial photodynamic therapy - what we know and what we don't, Crit. Rev. Microbiol. 44 (5) (2018) 571–589.
[17] S. Rajesh, et al., Antimicrobial photodynamic therapy: an overview, J. Indian Soc. Periodontol. 15 (4) (2011) 323–327.
[18] N.M. Idris, et al., In vivo photodynamic therapy using upconversion nanoparticles as remote-controlled nanotransducers, Nat. Med. 18 (10) (2012) 1580–1585.
[19] S. Son, et al., Multifunctional sonosensitizers in sonodynamic cancer therapy, Chem. Soc. Rev. 49 (11) (2020) 3244–3261.
[20] I. Rosenthal, J.Z. Sostaric, P. Riesz, Sonodynamic therapy–a review of the synergistic effects of drugs and ultrasound, Ultrason. Sonochem. 11 (6) (2004) 349–363.
[21] A.P. McHale, et al., Sonodynamic therapy: concept, mechanism and application to cancer treatment, Adv. Exp. Med. Biol. 880 (2016) 429–450.
[22] X. Wang, et al., Ultrafine titanium monoxide (TiO(1+x)) nanorods for enhanced sonodynamic therapy, J. Am. Chem. Soc. 142 (14) (2020) 6527–6537.
[23] X. Wang, et al., V-TiO2 nanospindles with regulating tumor microenvironment performance for enhanced sonodynamic cancer therapy, Appl. Phys. Rev. 7 (2020), 041411.
[24] X. Wang, et al., Liquid exfoliation of TiN nanodots as novel sonosensitizers for photothermal-enhanced sonodynamic therapy against cancer, Nano Today 39 (2021), 101170.
[25] S. Bai, et al., Ultrasmall iron-doped titanium oxide nanodots for enhanced sonodynamic and chemodynamic cancer therapy, ACS Nano 14 (11) (2020) 15119–15130.
[26] Q.L. Guo, et al., Nanosensitizers for sonodynamic therapy for glioblastoma multiforme: current progress and future perspectives, Mil Med Res 9 (1) (2022) 26.
[27] X. Qian, Y. Zheng, Y. Chen, Micro/nanoparticle-augmented sonodynamic therapy (SDT): breaking the depth shallow of photoactivation, Adv. Mater. 28 (37) (2016) 8097–8129.
[28] L. Serpe, F. Giuntini, Sonodynamic antimicrobial chemotherapy: first steps towards a sound approach for microbe inactivation, J. Photochem. Photobiol., B 150 (2015) 44–49.
[29] R. Wang, et al., Recent developments of sonodynamic therapy in antibacterial application, Nanoscale 14 (36) (2022) 12999–13017.
[30] N. Nomikou, et al., A versatile, stimulus-responsive nanoparticle-based platform for use in both sonodynamic and photodynamic cancer therapy, Acta Biomater. 49 (2017) 414–421.
[31] S. Shen, et al., Dual-core@shell-structured Fe(3)O(4)-NaYF(4)@TiO(2) nanocomposites as a magnetic targeting drug carrier for bioimaging and combined chemo-sonodynamic therapy, J. Mater. Chem. B 2 (35) (2014) 5775–5784.
[32] S. Liang, et al., Intelligent hollow Pt-CuS janus architecture for synergistic catalysis-enhanced sonodynamic and photothermal cancer therapy, Nano Lett. 19 (6) (2019) 4134–4145.
[33] W. Yue, et al., Checkpoint blockade and nanosonosensitizer-augmented noninvasive sonodynamic therapy combination reduces tumour growth and metastases in mice, Nat. Commun. 10 (1) (2019) 2025.
[34] X. Ma, et al., Ultrasound may be exploited for the treatment of microbial diseases, Med. Hypotheses 73 (1) (2009) 18–19.
[35] B. Liu, et al., The influence of ultrasound on the fluoroquinolones antibacterial activity, Ultrason. Sonochem. 18 (5) (2011) 1052–1056.
[36] F. Nakonechny, et al., Sonodynamic excitation of Rose Bengal for eradication of gram-positive and gram-negative bacteria, BioMed Res. Int. 2013 (2013), 684930.
[37] X. Lin, et al., Ultrasound-activated sensitizers and applications, Angew Chem. Int. Ed. Engl. 59 (34) (2020) 14212–14233.
[38] D.S. Benoit, H. Koo, Targeted, triggered drug delivery to tumor and biofilm microenvironments, Nanomedicine 11 (8) (2016) 873–879.
[39] Y. Su, et al., Recent advances in nanozymes for combating bacterial infection, Mater. Chem. Front. 6 (18) (2022) 2596–2609.
[40] Y. Hu, et al., Biofilm microenvironment-responsive nanoparticles for the treatment of bacterial infection, Nano Today 46 (2022), 101602.
[41] H. Hu, et al., Emerging nanomedicine-enabled/enhanced nanodynamic therapies beyond traditional photodynamics, Adv. Mater. 33 (12) (2021) e2005062.
[42] D.A. LaVan, T. McGuire, R. Langer, Small-scale systems for in vivo drug delivery, Nat. Biotechnol. 21 (10) (2003) 1184–1191.
[43] Q. Wu, et al., Surface wettability of nanoparticle modulated sonothrombolysis, Adv. Mater. 33 (25) (2021) e2007073.
[44] H.Y. Xu, et al., Nanoparticles in sonodynamic therapy: state of the art review, RSC Adv. 6 (56) (2016) 50697–50705.
[45] L. Fan, et al., Sonodynamic antimicrobial chemotherapy: an emerging alternative strategy for microbial inactivation, Ultrason. Sonochem. 75 (2021), 105591.
[46] M. Pourhajibagher, A. Bahador, Synergistic biocidal effects of metal oxide nanoparticles-assisted ultrasound irradiation: antimicrobial sonodynamic therapy against Streptococcus mutans biofilms, Photodiagnosis Photodyn. Ther. 35 (2021), 102432.
[47] Y. Zhu, et al., Rapid bacterial elimination achieved by sonodynamic Au@Cu(2)O hybrid nanocubes, Nanoscale 13 (37) (2021) 15699–15710.
[48] S.N. Shevchenko, et al., Antimicrobial effect of biocompatible silicon nanoparticles activated using therapeutic ultrasound, Langmuir 33 (10) (2017) 2603–2609.
[49] K. Su, et al., Rapid photo-sonotherapy for clinical treatment of bacterial infected bone implants by creating oxygen deficiency using sulfur doping, ACS Nano 14 (2) (2020) 2077–2089.
[50] X. Bi, et al., Silver peroxide nanoparticles for combined antibacterial sonodynamic and photothermal therapy, Small 18 (2) (2022) e2104160.
[51] M. Pourhajibagher, et al., The anti-biofilm capability of nano-emodin-mediated sonodynamic therapy on multi-species biofilms produced by burn wound bacterial strains, Photodiagnosis Photodyn. Ther. 34 (2021), 102288.

[52] X. Pang, et al., Bacteria-responsive nanoliposomes as smart sonotheranostics for multidrug resistant bacterial infections, ACS Nano 13 (2) (2019) 2427–2438.
[53] X. Pang, et al., Sono-immunotherapeutic nanocapturer to combat multidrug-resistant bacterial infections, Adv. Mater. 31 (35) (2019) e1902530.
[54] M. Yang, et al., The synergistic fungicidal effect of low-frequency and low-intensity ultrasound with amphotericin B-loaded nanoparticles on C. albicans in vitro, Int. J. Pharm. 542 (1–2) (2018) 232–241.
[55] M. Pourhajibagher, B. Pourakbari, A. Bahador, Contribution of antimicrobial photo-sonodynamic therapy in wound healing: an in vivo effect of curcumin-nisin-based poly (L-lactic acid) nanoparticle on Acinetobacter baumannii biofilms, BMC Microbiol. 22 (1) (2022) 28.
[56] M. Pourhajibagher, et al., Photo-sonodynamic antimicrobial chemotherapy via chitosan nanoparticles-indocyanine green against polymicrobial periopathogenic biofilms: ex vivo study on dental implants, Photodiagnosis Photodyn. Ther. 31 (2020), 101834.
[57] X. Geng, et al., Oxygen-carrying biomimetic nanoplatform for sonodynamic killing of bacteria and treatment of infection diseases, Ultrason. Sonochem. 84 (2022), 105972.
[58] Y. Yu, et al., Single-atom catalysis for efficient sonodynamic therapy of methicillin-resistant Staphylococcus aureus-infected osteomyelitis, ACS Nano 15 (6) (2021) 10628–10639.
[59] D. Sun, et al., Ultrasound-switchable nanozyme augments sonodynamic therapy against multidrug-resistant bacterial infection, ACS Nano 14 (2) (2020) 2063–2076.
[60] J. Guo, et al., An MSN-based synergistic nanoplatform for root canal biofilm eradication via Fenton-enhanced sonodynamic therapy, J. Mater. Chem. B 9 (37) (2021) 7686–7697.
[61] B. Huang, et al., IR780 based sonotherapeutic nanoparticles to combat multidrug-resistant bacterial infections, Front. Chem. 10 (2022), 840598.
[62] M. Pourhajibagher, et al., Sonodynamic excitation of nanomicelle curcumin for eradication of Streptococcus mutans under sonodynamic antimicrobial chemotherapy: enhanced anti-caries activity of nanomicelle curcumin, Photodiagnosis Photodyn. Ther. 30 (2020), 101780.
[63] D. Wang, et al., Precise magnetic resonance imaging-guided sonodynamic therapy for drug-resistant bacterial deep infection, Biomaterials 264 (2021), 120386.
[64] Z. Wang, et al., Photomagnetic nanoparticles in dual-modality imaging and photo-sonodynamic activity against bacteria, Chem. Eng. J. 356 (2019) 811–818.
[65] M. Tarhini, H. Greige-Gerges, A. Elaissari, Protein-based nanoparticles: from preparation to encapsulation of active molecules, Int. J. Pharm. 522 (1–2) (2017) 172–197.
[66] Y. Wang, et al., Preparation of sonoactivated TiO(2)-DVDMS nanocomposite for enhanced antibacterial activity, Ultrason. Sonochem. 63 (2020), 104968.
[67] T.J. Silhavy, D. Kahne, S. Walker, The bacterial cell envelope, Cold Spring Harbor Perspect. Biol. 2 (5) (2010) a000414.
[68] U. Chilakamarthi, L. Giribabu, Photodynamic therapy: past, present and future, Chem. Rec. 17 (8) (2017) 775–802.
[69] G. Jori, et al., Photodynamic therapy in the treatment of microbial infections: basic principles and perspective applications, Laser Surg. Med. 38 (5) (2006) 468–481.
[70] X. Pang, et al., Beyond antibiotics: photo/sonodynamic approaches for bacterial theranostics, Nano-Micro Lett. 12 (1) (2020) 144.
[71] V. Choi, M.A. Rajora, G. Zheng, Activating drugs with sound: mechanisms behind sonodynamic therapy and the role of nanomedicine, Bioconjugate Chem. 31 (4) (2020) 967–989.
[72] Y. Liu, et al., Antibacterial photodynamic therapy: overview of a promising approach to fight antibiotic-resistant bacterial infections, J Clin Transl Res 1 (3) (2015) 140–167.
[73] L. Brovko, Photodynamic treatment: a new efficient alternative for surface sanitation, Adv. Food Nutr. Res. 61 (2010) 119–147.
[74] V.S. Ghate, W. Zhou, H.G. Yuk, Perspectives and trends in the application of photodynamic inactivation for microbiological food safety, Compr. Rev. Food Sci. Food Saf. 18 (2) (2019) 402–424.
[75] D. Ma, et al., Effects of acoustic streaming from moderate-intensity pulsed ultrasound for enhancing biofilm mitigation effectiveness of drug-loaded liposomes, J. Acoust. Soc. Am. 138 (2) (2015) 1043–1051.
[76] Y. Li, et al., A multifunctional Fenton nanoagent for microenvironment-selective anti-biofilm and anti-inflammatory therapy, Mater. Horiz. 8 (4) (2021) 1264–1271.
[77] Z. Wang, et al., Infection microenvironment-related antibacterial nanotherapeutic strategies, Biomaterials 280 (2022), 121249.
[78] Q. Wang, et al., Therapeutic applications of antimicrobial silver-based biomaterials in dentistry, Int. J. Nanomed. 17 (2022) 443–462.
[79] J. Wu, W.L. Nyborg, Ultrasound, cavitation bubbles and their interaction with cells, Adv. Drug Deliv. Rev. 60 (10) (2008) 1103–1116.
[80] S. Kwiatkowski, et al., Photodynamic therapy - mechanisms, photosensitizers and combinations, Biomed. Pharmacother. 106 (2018) 1098–1107.
[81] M. Niedre, M.S. Patterson, B.C. Wilson, Direct near-infrared luminescence detection of singlet oxygen generated by photodynamic therapy in cells in vitro and tissues in vivo, Photochem. Photobiol. 75 (4) (2002) 382–391.
[82] N. Bhargava, et al., Advances in application of ultrasound in food processing: a review, Ultrason. Sonochem. 70 (2021), 105293.
[83] M. Trendowski, The promise of sonodynamic therapy, Cancer Metastasis Rev. 33 (1) (2014) 143–160.
[84] M.J. Pickworth, et al., Studies of the cavitational effects of clinical ultrasound by sonoluminescence: 4. The effect of therapeutic ultrasound on cells in monolayer culture in a standing wave field, Phys. Med. Biol. 34 (11) (1989) 1553–1560.
[85] T.K. Saksena, Sonoluminescence from stable cavitation, J. Chem. Phys. 53 (5) (1970) 1722–&.
[86] K.T. Byun, K.Y. Kim, H.Y. Kwak, Sonoluminescence characteristics from micron and submicron bubbles, J. Kor. Phys. Soc. 47 (6) (2005) 1010–1022.
[87] L. Rengeng, et al., Sonodynamic therapy, a treatment developing from photodynamic therapy, Photodiagnosis Photodyn. Ther. 19 (2017) 159–166.
[88] V. Misík, P. Riesz, Free radical intermediates in sonodynamic therapy, Ann. N. Y. Acad. Sci. 899 (2000) 335–348.
[89] J. Wang, et al., Magneto-based synergetic therapy for implant-associated infections via biofilm disruption and innate immunity regulation, Adv. Sci. 8 (6) (2021), 2004010.
[90] Z. Yuan, et al., Near-infrared light-triggered nitric-oxide-enhanced photodynamic therapy and low-temperature photothermal therapy for biofilm elimination, ACS Nano 14 (3) (2020) 3546–3562.
[91] Y. Zhang, et al., Nanobiotechnology-enabled energy utilization elevation for augmenting minimally-invasive and noninvasive oncology thermal ablation, Wiley Interdiscip Rev Nanomed Nanobiotechnol 13 (6) (2021) e1733.
[92] B. Hu, et al., Thermal-disrupting interface mitigates intercellular cohesion loss for accurate topical antibacterial therapy, Adv. Mater. 32 (12) (2020) e1907030.
[93] X. Pan, et al., Sonodynamic therapy (SDT): a novel strategy for cancer nanotheranostics, Sci. China Life Sci. 61 (4) (2018) 415–426.
[94] Ritenour et al., Ultrasound: Its Chemical, Physical, and Biological Effects, Radiology 173(1)(1989) 136-136.
[95] H. Chen, et al., Recent progress in development of new sonosensitizers for sonodynamic cancer therapy, Drug Discov. Today 19 (4) (2014) 502–509.
[96] R.A. Hiller, S.J. Putterman, K.R. Weninger, Time-resolved spectra of sonoluminescence, Phys. Rev. Lett. 80 (5) (1998) 1090–1093.
[97] P.R. Gogate, A.M. Kabadi, A review of applications of cavitation in biochemical engineering/biotechnology, Biochem. Eng. J. 44 (1) (2009) 60–72.
[98] Y. Yang, et al., Mechanisms underlying sonoporation: interaction between microbubbles and cells, Ultrason. Sonochem. 67 (2020), 105096.
[99] L. Zhang, et al., Sonophotocatalytic inactivation of E. coli using ZnO nanofluids and its mechanism, Ultrason. Sonochem. 34 (2017) 232–238.
[100] X.W. Wang, et al., Newly developed strategies for improving sonodynamic therapy, Mater. Horiz. 7 (8) (2020) 2028–2046.
[101] I.K. Herrmann, How nanotechnology-enabled concepts could contribute to the prevention, diagnosis and therapy of bacterial infections, Crit. Care 19 (1) (2015) 239.
[102] A. Axer, et al., Harnessing the maltodextrin transport mechanism for targeted bacterial imaging: structural requirements for improved in vivo stability in tracer design, ChemMedChem 13 (3) (2018) 241–250.
[103] P. Kennedy, et al., biofilm and a new appraisal of burn wound sepsis, Burns 36 (1) (2010) 49–56.
[104] S. Asati, U. Chaudhary, Prevalence of biofilm producing aerobic bacterial isolates in burn wound infections at a tertiary care hospital in northern India, Ann Burns Fire Disasters 30 (1) (2017) 39–42.
[105] W. Xiu, et al., Recent development of nanomedicine for the treatment of bacterial biofilm infections, View 2 (1) (2020), 20200065.
[106] H.C. Flemming, et al., Biofilms: an emergent form of bacterial life, Nat. Rev. Microbiol. 14 (9) (2016) 563–575.
[107] H. Koo, et al., Targeting microbial biofilms: current and prospective therapeutic strategies, Nat. Rev. Microbiol. 15 (12) (2017) 740–755.
[108] Y. Zhu, et al., Rapid bacterial elimination achieved by sonodynamic Au@Cu(2)O hybrid nanocubes, Nanoscale 13 (2021) 15699–15710.
[109] H. Dong, et al., Biofilm microenvironment response nanoplatform synergistically degrades biofilm structure and relieves hypoxia for efficient sonodynamic therapy, Chem. Eng. J. 453 (2023), 139839.
[110] Y.M. You, et al., An organic-inorganic perovskite ferroelectric with large piezoelectric response, Science 357 (6348) (2017) 306–309.
[111] M. Wu, et al., Piezoelectric nanocomposites for sonodynamic bacterial elimination and wound healing, Nano Today 37 (2021), 101104.
[112] H.F. Jenkinson, R.J. Lamont, Oral microbial communities in sickness and in health, Trends Microbiol. 13 (12) (2005) 589–595.
[113] N. Zhou, et al., Microbiota analysis of peri-implant mucositis in patients with periodontitis history, Clin. Oral Invest. 26 (10) (2022) 6223–6233.
[114] S. Moosavi Nejad, et al., Acute effects of sono-activated photocatalytic titanium dioxide nanoparticles on oral squamous cell carcinoma, Ultrason. Sonochem. 32 (2016) 95–101.
[115] Y. Lv, et al., Antiproliferative and apoptosis-inducing effect of exo-protoporphyrin IX based sonodynamic therapy on human oral squamous cell carcinoma, Sci. Rep. 7 (2017), 40967.
[116] M. Lafond, S. Yoshizawa, S.I. Umemura, Sonodynamic therapy: advances and challenges in clinical translation, J. Ultrasound Med. 38 (3) (2019) 567–580.
[117] L. Jiang, et al., Sonodynamic therapy in atherosclerosis by curcumin nanosuspensions: preparation design, efficacy evaluation, and mechanisms analysis, Eur. J. Pharm. Biopharm. 146 (2020) 101–110.
[118] R.H. Selwitz, A.I. Ismail, N.B. Pitts, Dental caries, Lancet 369 (9555) (2007) 51–59.
[119] D.P. Lew, F.A. Waldvogel, *Osteomyelitis.* Lancet 364 (9431) (2004) 369–379.
[120] A. Widaa, et al., Staphylococcus aureus protein A plays a critical role in mediating bone destruction and bone loss in osteomyelitis, PLoS One 7 (7) (2012), e40586.
[121] A.L. Lima, et al., Recommendations for the treatment of osteomyelitis, Braz. J. Infect. Dis. 18 (5) (2014) 526–534.
[122] D.C. Bury, T.S. Rogers, M.M. Dickman, Osteomyelitis: diagnosis and treatment, Am. Fam. Physician 104 (4) (2021) 395–402.

[123] X. Feng, et al., Piezo-augmented sonosensitizer with strong ultrasound-propelling ability for efficient treatment of osteomyelitis, ACS Nano 16 (2) (2022) 2546–2557.
[124] J. Lei, et al., Sulfur-regulated defect engineering for enhanced ultrasonic piezocatalytic therapy of bacteria-infected bone defects, Chem. Eng. J. 435 (2022), 134624.
[125] N.F. Crum-Cianflone, Bacterial, fungal, parasitic, and viral myositis, Clin. Microbiol. Rev. 21 (3) (2008) 473–494.
[126] S.A. Greenberg, Inflammatory myopathies: disease mechanisms, Curr. Opin. Neurol. 22 (5) (2009) 516–523.
[127] M. Qi, et al., Novel nanomaterial-based antibacterial photodynamic therapies to combat oral bacterial biofilms and infectious diseases, Int. J. Nanomed. 14 (2019) 6937–6956.
[128] F. Xu, et al., Yolk-structured multifunctional up-conversion nanoparticles for synergistic photodynamic-sonodynamic antibacterial resistance therapy, Biomater. Sci. 5 (4) (2017) 678–685.
[129] J. Derks, et al., Peri-implantitis - onset and pattern of progression, J. Clin. Periodontol. 43 (4) (2016) 383–388.
[130] J.W. Xu, K. Yao, Z.K. Xu, Nanomaterials with a photothermal effect for antibacterial activities: an overview, Nanoscale 11 (18) (2019) 8680–8691.
[131] I. de Miguel, et al., Plasmon-based biofilm inhibition on surgical implants, Nano Lett. 19 (4) (2019) 2524–2529.
[132] J. Huo, et al., Emerging photothermal-derived multimodal synergistic therapy in combating bacterial infections, Chem. Soc. Rev. 50 (15) (2021) 8762–8789.
[133] T. Ibelli, S. Templeton, N. Levi-Polyachenko, Progress on utilizing hyperthermia for mitigating bacterial infections, Int. J. Hyperther. 34 (2) (2018) 144–156.
[134] R.X. Toh, et al., Debridement, antibiotics, and implant retention in periprosthetic joint infection: what predicts success or failure? J. Arthroplasty 36 (10) (2021) 3562–3569.
[135] E.T. Rochford, R.G. Richards, T.F. Moriarty, Influence of material on the development of device-associated infections, Clin. Microbiol. Infect. 18 (12) (2012) 1162–1167.
[136] L. Tan, et al., Rapid biofilm eradication on bone implants using red phosphorus and near-infrared light, Adv. Mater. 30 (31) (2018) e1801808.
[137] S.D. Goodman, et al., Biofilms can be dispersed by focusing the immune system on a common family of bacterial nucleoid-associated proteins, Mucosal Immunol. 4 (6) (2011) 625–637.
[138] F. Cavalieri, et al., Nanomedicines for antimicrobial interventions, J. Hosp. Infect. 88 (4) (2014) 183–190.
[139] R.H. Fang, et al., Engineered nanoparticles mimicking cell membranes for toxin neutralization, Adv. Drug Deliv. Rev. 90 (2015) 69–80.
[140] S.W. Dickey, G.Y.C. Cheung, M. Otto, Different drugs for bad bugs: antivirulence strategies in the age of antibiotic resistance, Nat. Rev. Drug Discov. 16 (7) (2017) 457–471.
[141] M. Liang, et al., Ultrasound activatable microneedles for bilaterally augmented sono-chemodynamic and sonothermal antibacterial therapy, Acta Biomater S1742-7061(22) (2022) 00851.
[142] V. Naddeo, et al., Water and wastewater disinfection by ultrasound irradiation- a critical review, Global Nest Journal 16 (2014) 561–577.
[143] Y. Zhang, et al., Hematoporphyrin monomethyl ether mediated sonodynamic antimicrobial chemotherapy on porphyromonas gingivalis in vitro, Microb. Pathog. 144 (2020), 104192.
[144] D. Zhuang, et al., Sonodynamic effects of hematoporphyrin monomethyl ether on Staphylococcus aureus in vitro, FEMS Microbiol. Lett. 361 (2) (2014) 174–180.
[145] X. Ding, et al., Biodegradable antibacterial polymeric nanosystems: a new hope to cope with multidrug-resistant bacteria, Small 15 (20) (2019) e1900999.